



Overview of Optical Metrology of Advanced Semiconductor Materials

Vimal K. Kamineni

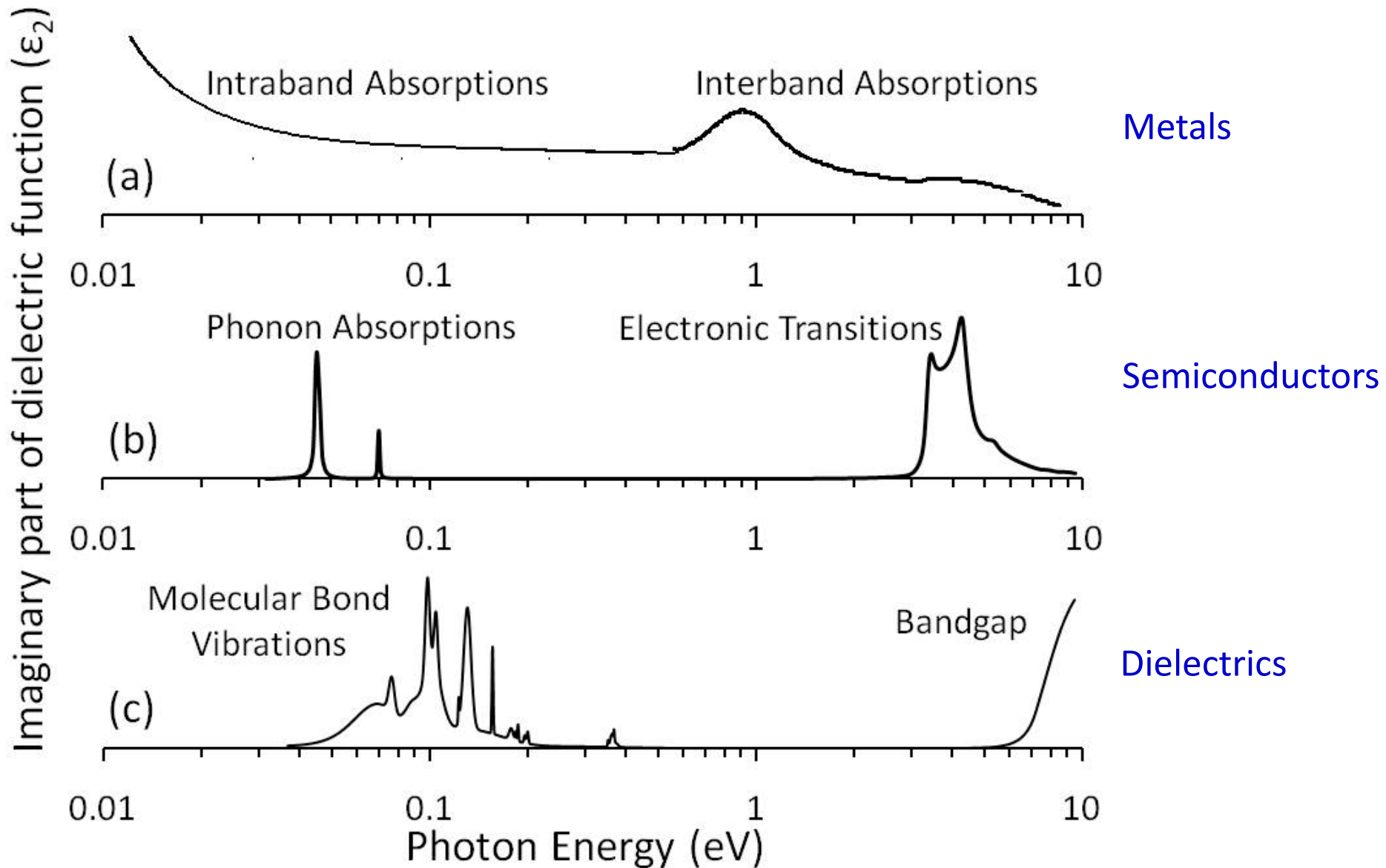
College of Nanoscale Science and Engineering,

University at Albany – SUNY, Albany, NY 12203

May 25, 2011



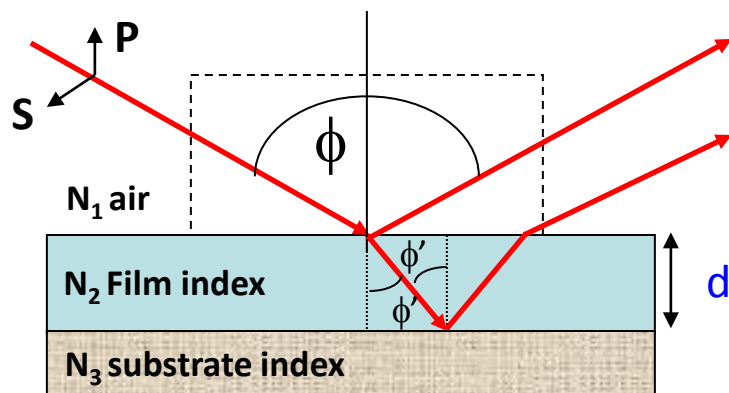
- Linear Optical Response of Materials
- Spectroscopic Ellipsometry
- Advanced Materials in the Semiconductor Industry
- Photoreflectance
- Photoluminescence
- Conclusions
- Acknowledgements





Spectroscopic Ellipsometry: Light polarized in plane of reflection reflects differently than light polarized perpendicular to plane of reflection.

Reflection of Polarized Light



$$\beta = 2\pi(d/\lambda)N_2 \cos \phi'$$

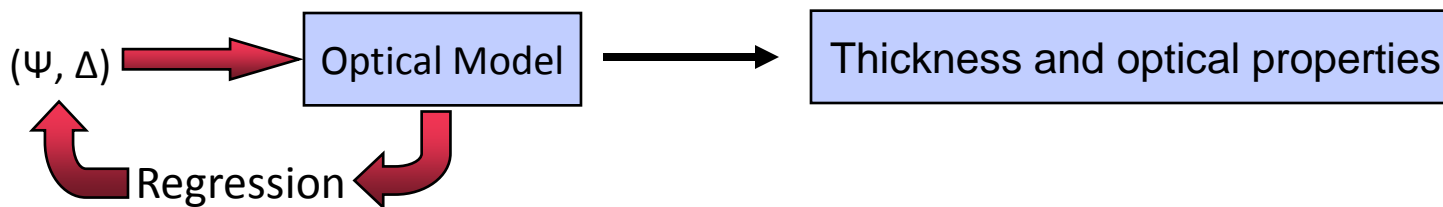
Fresnel Reflection Coefficients different for S and P polarizations

$$r_{12}^P = \frac{N_2 \cos \phi - N_1 \cos \phi'}{N_2 \cos \phi + N_1 \cos \phi'} \quad r_{12}^S = \frac{N_1 \cos \phi - N_2 \cos \phi'}{N_2 \cos \phi + N_1 \cos \phi'}$$

$$R^P = \frac{r_{12}^P + r_{23}^P e^{-i2\beta}}{1 + r_{12}^P r_{23}^P e^{-i2\beta}} \quad R^S = \frac{r_{12}^S + r_{23}^S e^{-i2\beta}}{1 + r_{12}^S r_{23}^S e^{-i2\beta}}$$

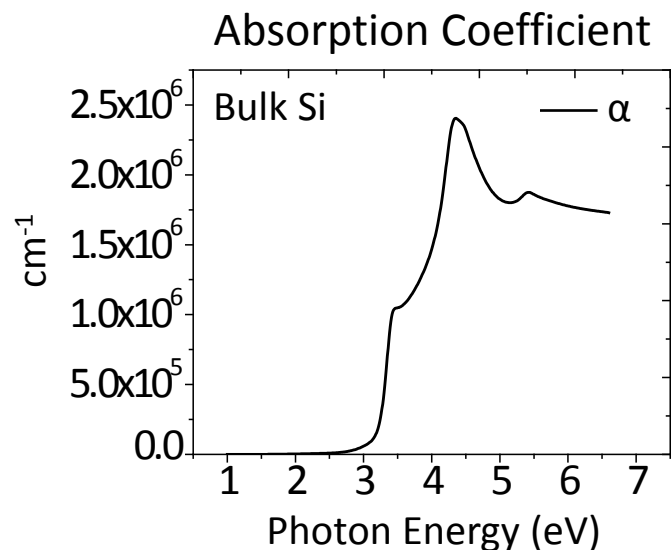
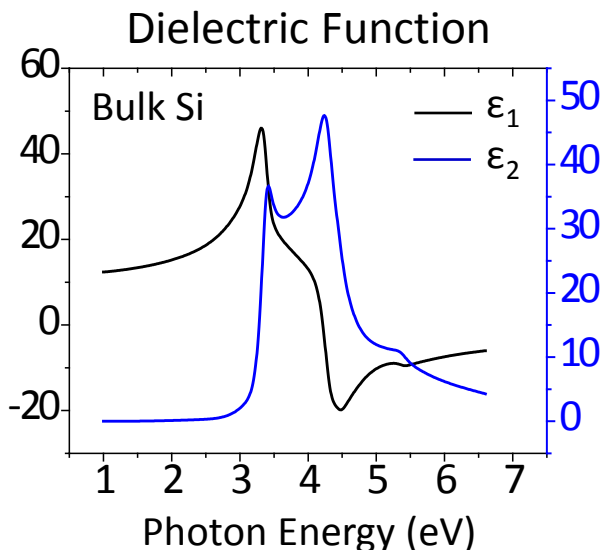
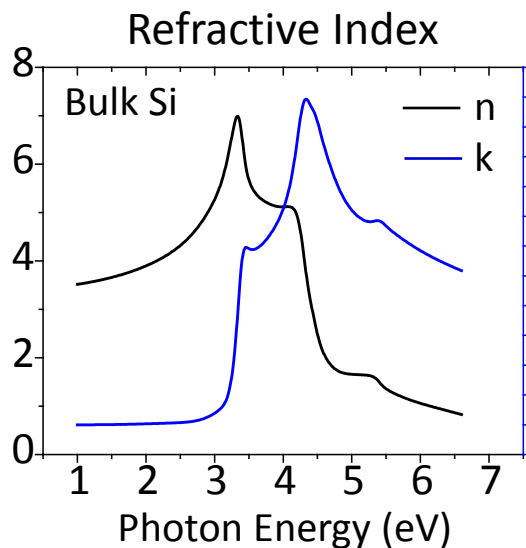
$$\tan \Psi e^{i\Delta} = \frac{R^P}{R^S}$$

$$\Psi = \tan^{-1} \left(\frac{|R^P|}{|R^S|} \right), \Delta = \delta_i - \delta_r$$

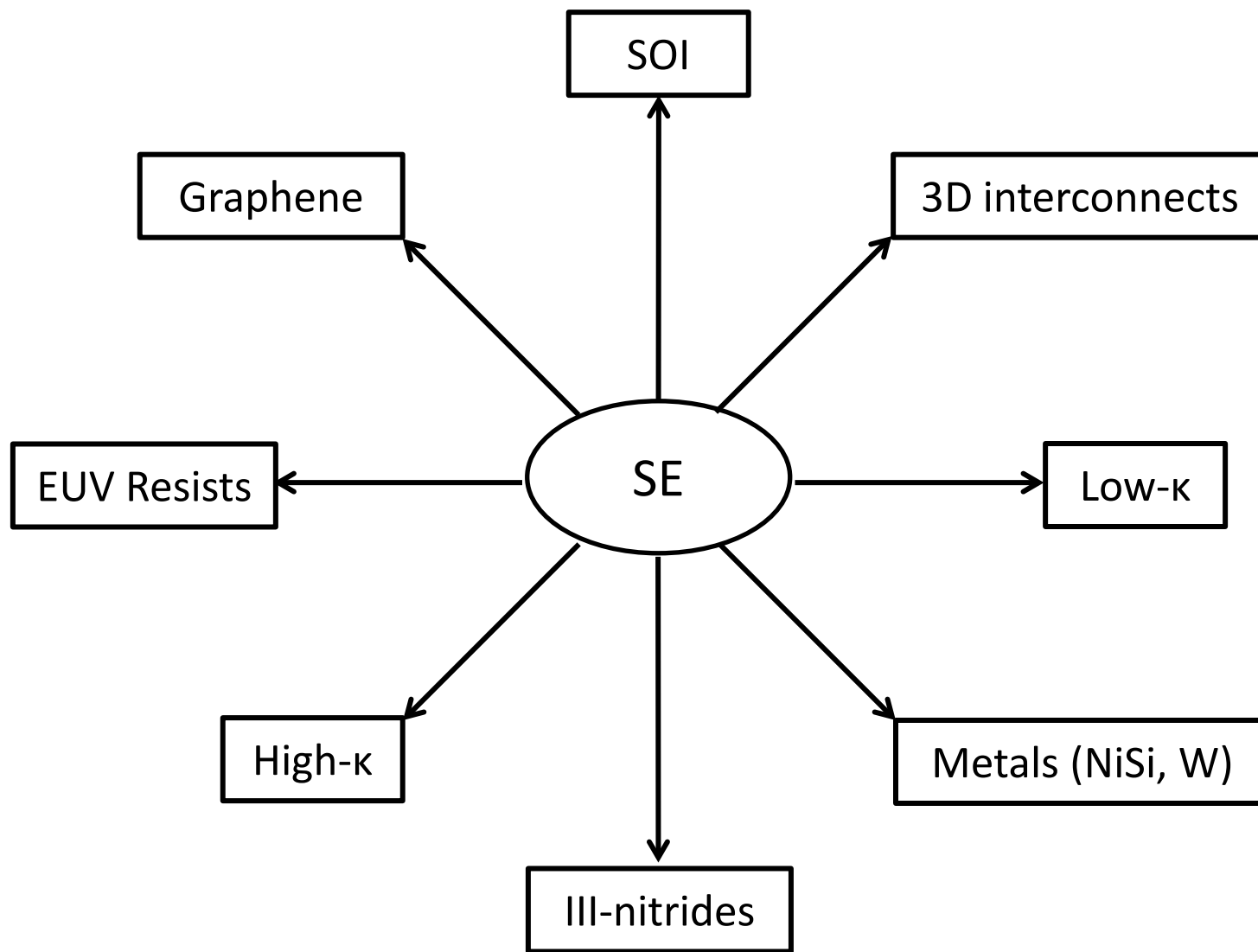


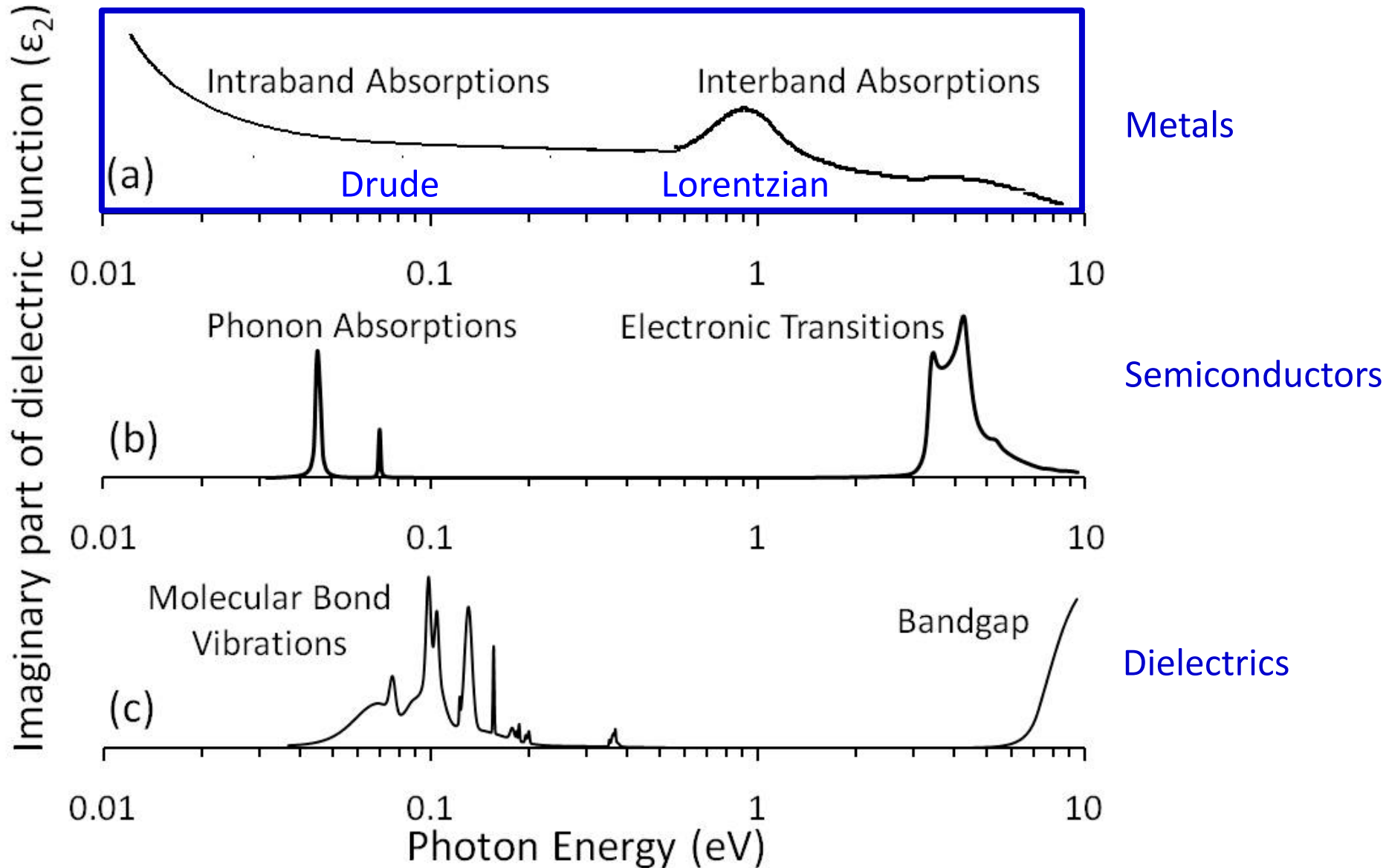
$$\tilde{\epsilon} = \epsilon_1 + i\epsilon_2 = (\tilde{N})^2 = (n + ik)^2 = (n^2 - k^2) + 2ink$$

$$\alpha = \frac{4\pi k}{\lambda}$$



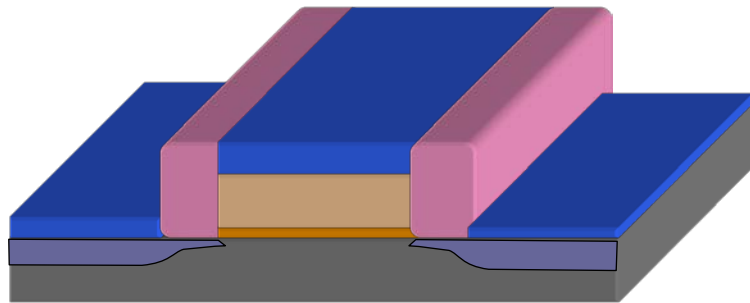
Ψ - amplitude ratio, Δ - phase difference, R - Fresnel reflection coefficient, n - real part of the refractive index, k - extinction coefficient, ϵ_1 - real part of the dielectric function, ϵ_2 - imaginary part of the dielectric function, α - absorption coefficient, λ - wavelength of light.







Optical Metrology of thin metal films (Ni, NiSi, TiN and W)



-  Poly-Si Gate Electrode
-  Thermal SiO₂
-  Nitride Spacer
-  Nickel Silicide
-  N⁺ Doped Silicon Source Drain
-  P well

V.K. Kamineni, M. Raymond, E.J. Bersch, B.B. Doris, and A.C. Diebold, Journal of Applied Physics, 107 (2010) 093525.



SE Methods & Limitations

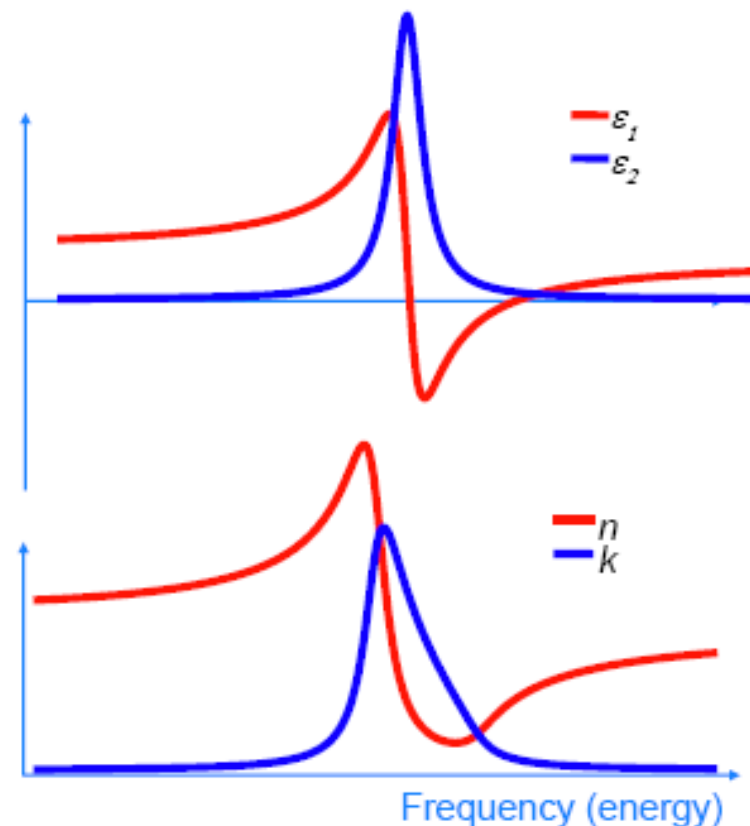
$$\text{VUV VASE} \implies \frac{r_p}{r_s} = (\tan \psi) e^{i\Delta} \implies \psi \ \& \ \Delta \implies n, k \ \& \ t$$

- ✓ Transparent
- ✓ Semi-absorbing film
- x Absorbing

- Interference enhancements measurements (angle)
- Transmission intensity
- *In situ* measurements
- Optical constant parameterization

$$\tilde{n} = n - ik \implies \text{Kramers-Kronig Consistency}$$

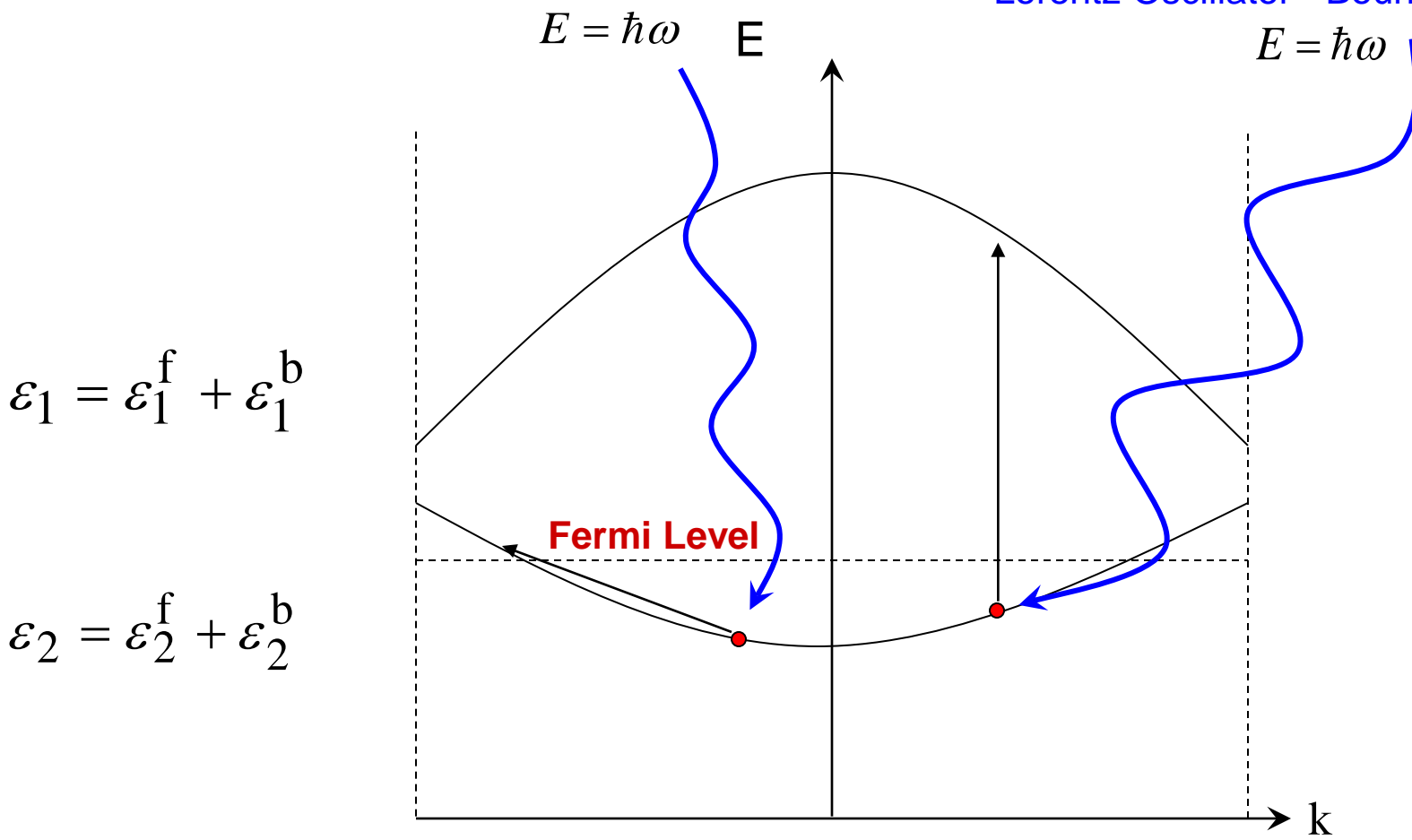
$$\varepsilon_1 + i\varepsilon_2 = (n - ik)^2$$





Drude Oscillator - Free Electron

Lorentz Oscillator - Bound Electron





Optical model for metals

$$\epsilon_1 = \epsilon_\infty + \omega_{pb}^2 \frac{\tau_b^2 (\omega_o^2 - \omega^2)}{\tau_b^2 (\omega_o^2 - \omega^2)^2 + \omega^2} - \omega_{pf}^2 \frac{\tau_f^2}{\tau_f^2 \omega^2 + 1}$$

$$\epsilon_2 = \epsilon_\infty + \omega_{pb}^2 \frac{\tau_b \omega}{\tau_b^2 (\omega_o^2 - \omega^2)^2 + \omega^2} + \omega_{pf}^2 \frac{\tau_f}{\omega (\tau_f^2 \omega^2 + 1)}$$

From Ellipsometry you can extract τ_f

Mayadas and Shatzkes -

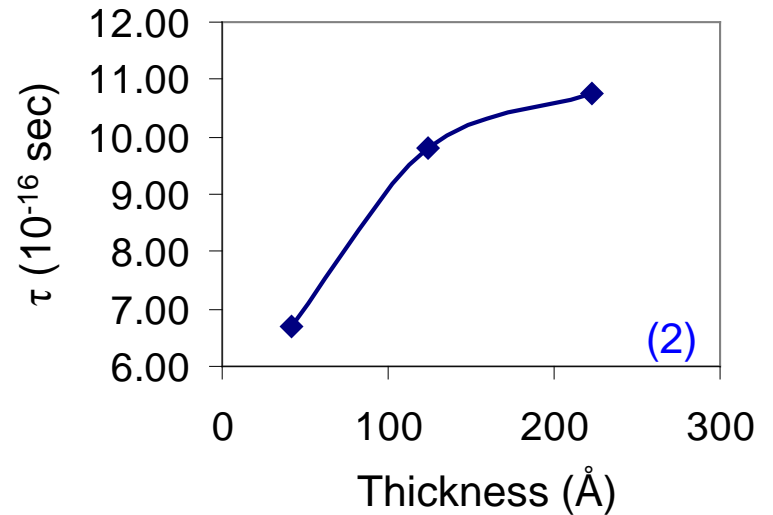
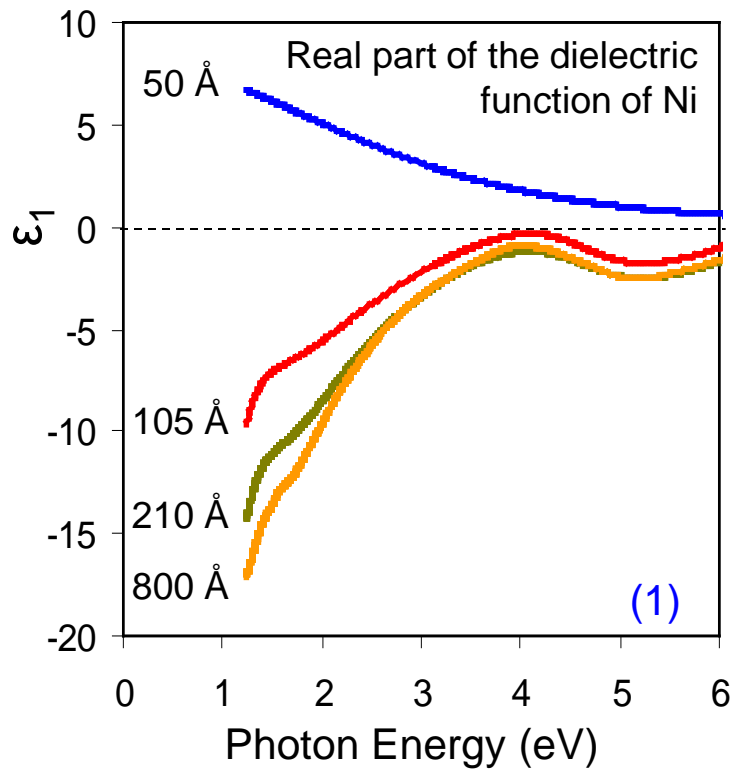
$$\frac{1}{\tau_f} = \frac{1}{\tau_{bulk}} + \frac{v_F}{\lambda} \quad \longrightarrow \quad \lambda = \left[\frac{2(1 - \mathfrak{R})}{3\mathfrak{R}} \right] R_g$$

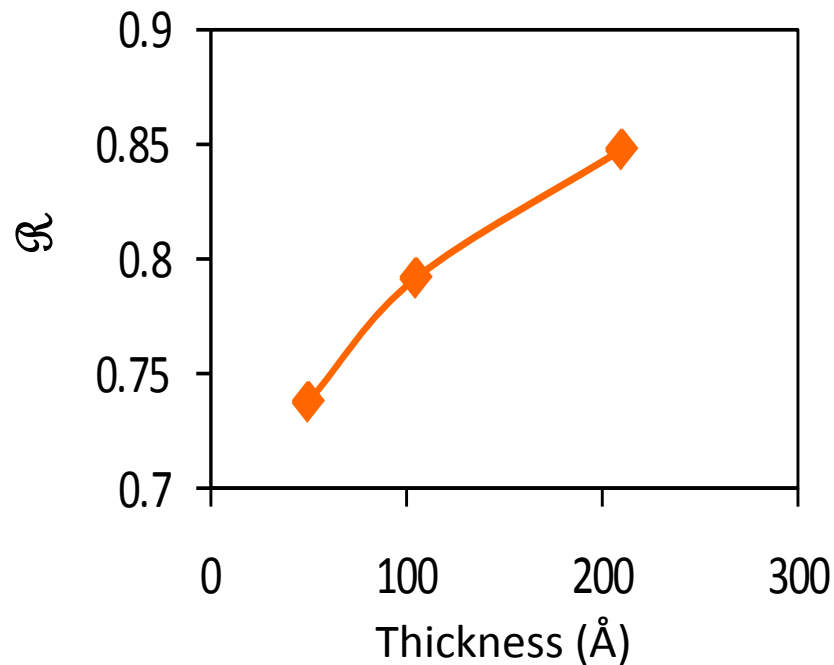
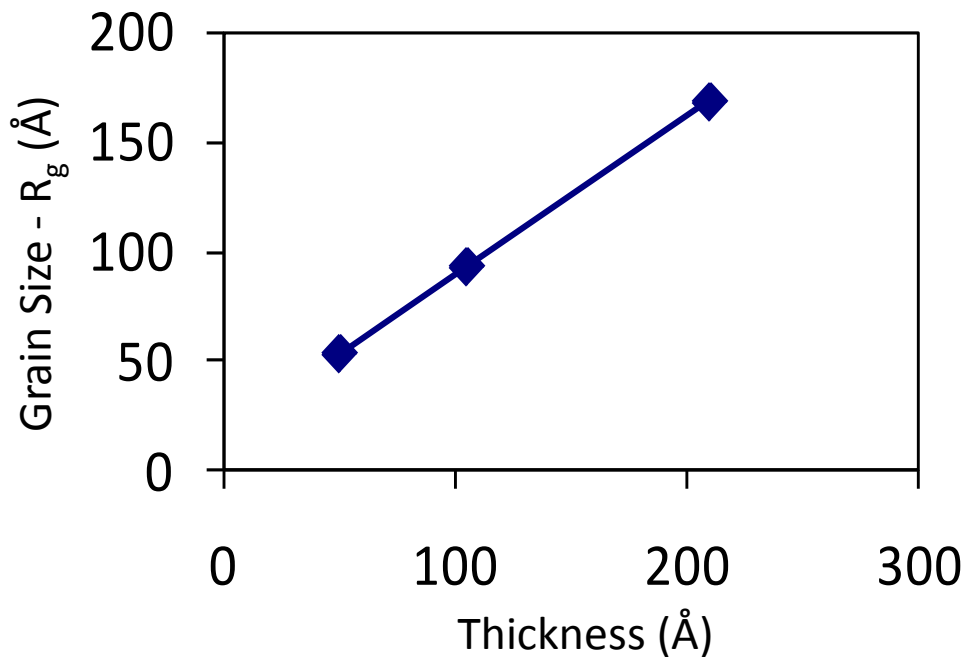


Mayadas and Shatzkes

$$\frac{1}{\tau_f} = \frac{1}{\tau_{bulk}} + \frac{v_F}{\lambda}$$

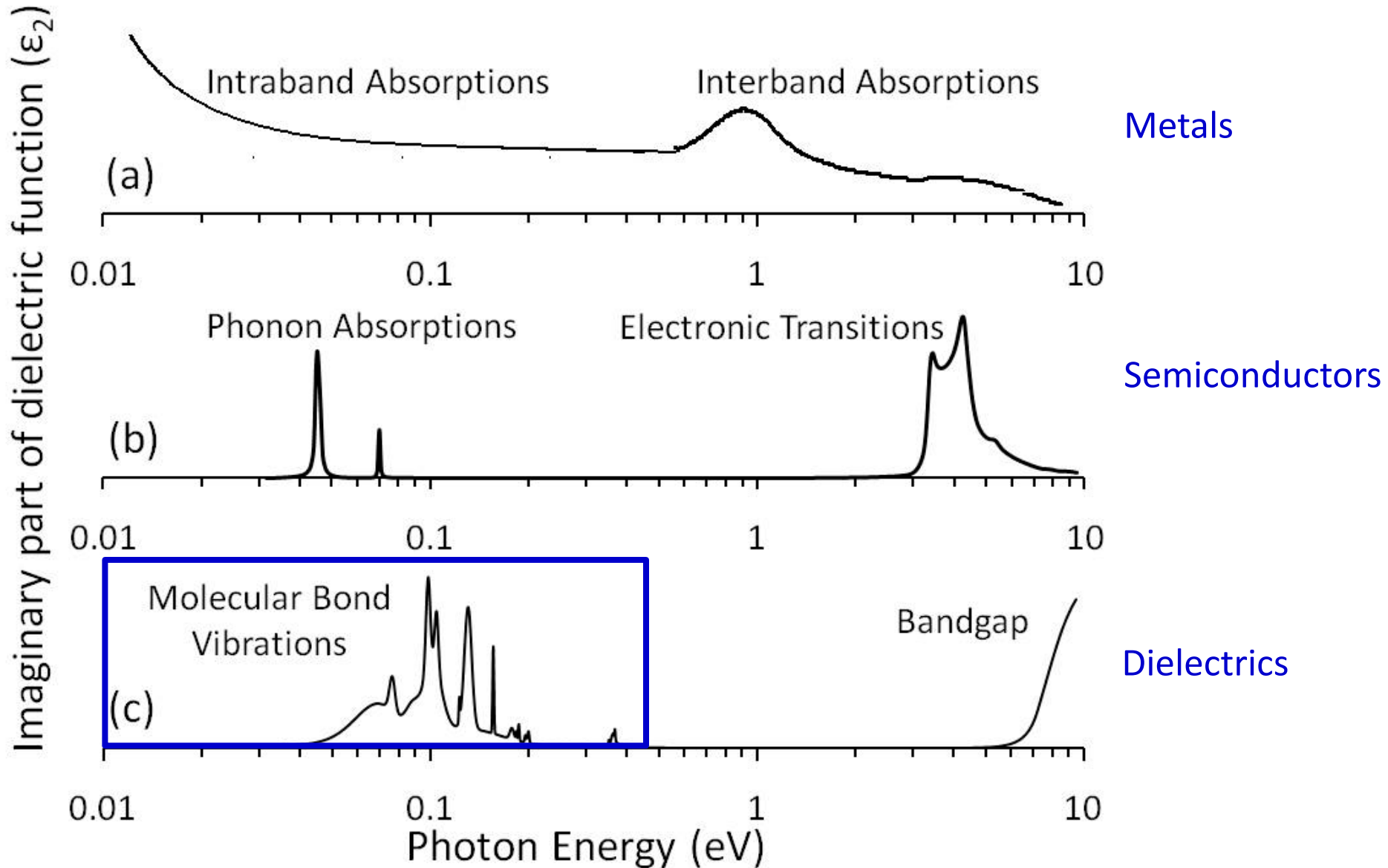
$$\lambda = \left[\frac{2(1 - \mathfrak{R})}{3\mathfrak{R}} \right] R_g$$





Conclusions

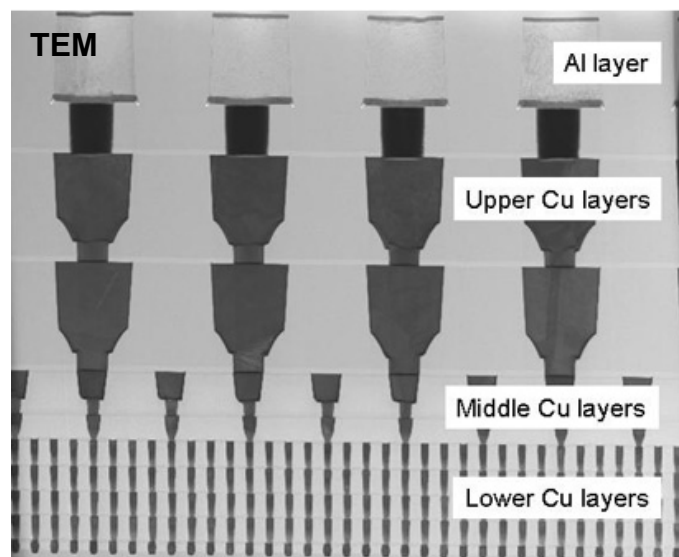
1. An Optical model was developed to determine the thickness of thin metal films.
2. Model was built to show that the thickness-dependent optical properties of thin metal films are correlated to the change in Drude free electron relaxation time.
3. The change in free electron relaxation time was traced to the change in grain boundary reflection coefficient and grain size.



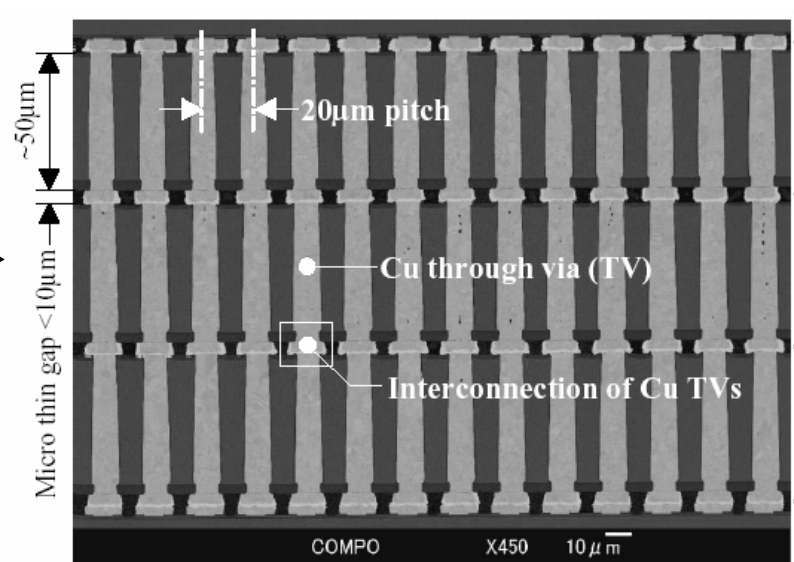


Investigation of Optical Properties of BCB Wafer Bonding Layer used for 3D Interconnects via Infrared Spectroscopic Ellipsometry

2D Interconnects – 45 nm node



3D Interconnects – TSV

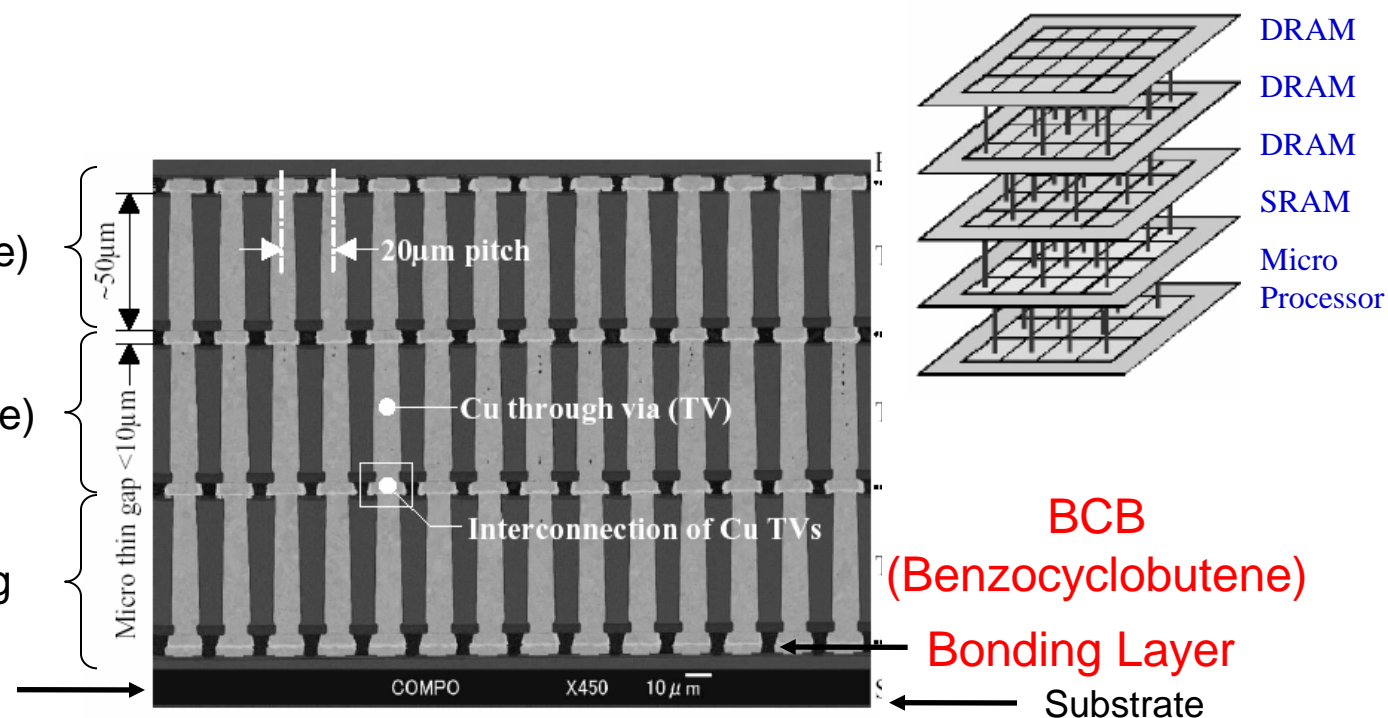


V.K. Kamineni, P. Singh, L.-W. Kong, J. Hudnall, J. Qureshi, C. Taylor, A. Rudack, S. Arkalgud, and A.C. Diebold, *Thin Solid Films*, 519 (2011) 2924.

P. Singh, J. Hudnall, J. Qureshi, V.K. Kamineni, C. Taylor, A. Rudack, A. Diebold and S. Arkalgud, *Mater. Res. Soc. Symp. Proc.*, 1249 (2010) 309.

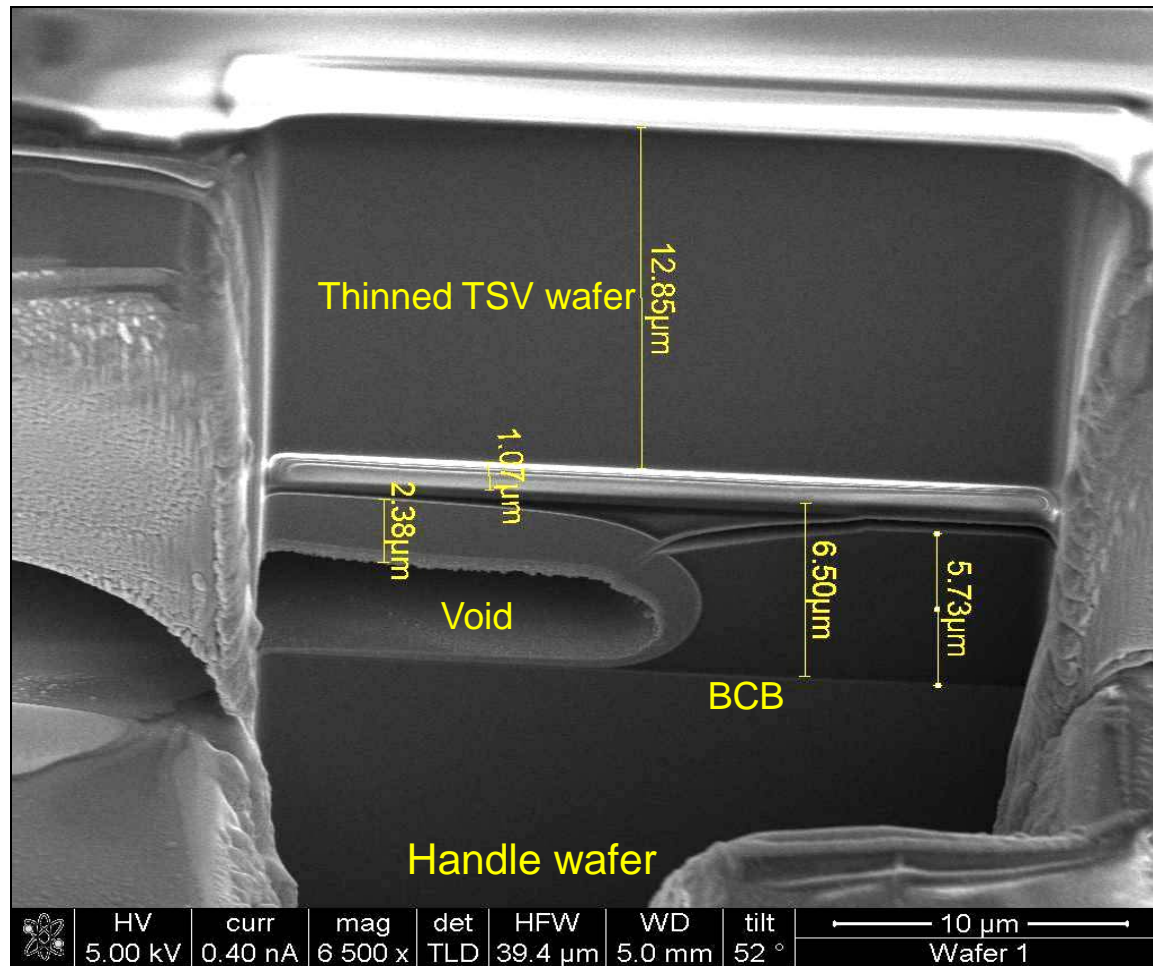


- Replacing long horizontal lines with short vertical interconnects
 - Addresses RC delay, crosstalk and power consumption
- Enables integration of heterogeneous devices & technologies (memory, logic, RF, analog, sensors)
 - Enables new functionalities
 - Cost reduction compared to SoC



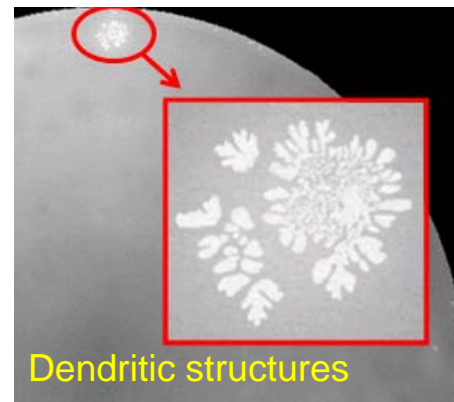
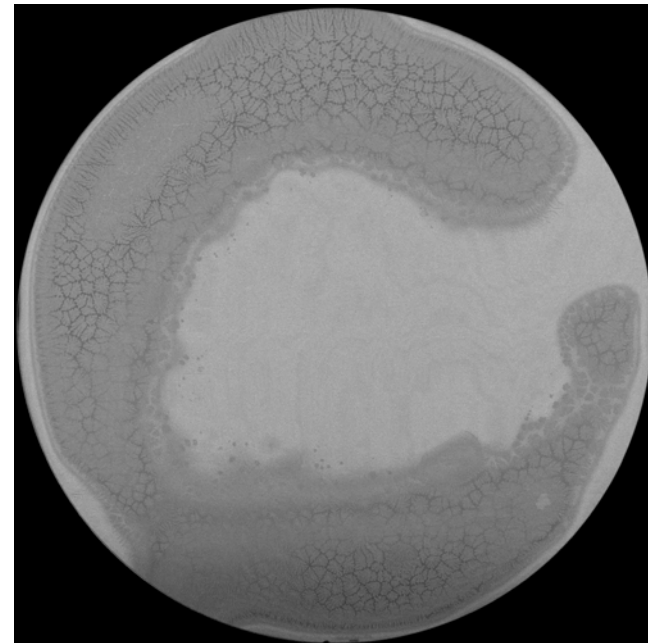


Top wafer peeling due to air pockets in the BCB film



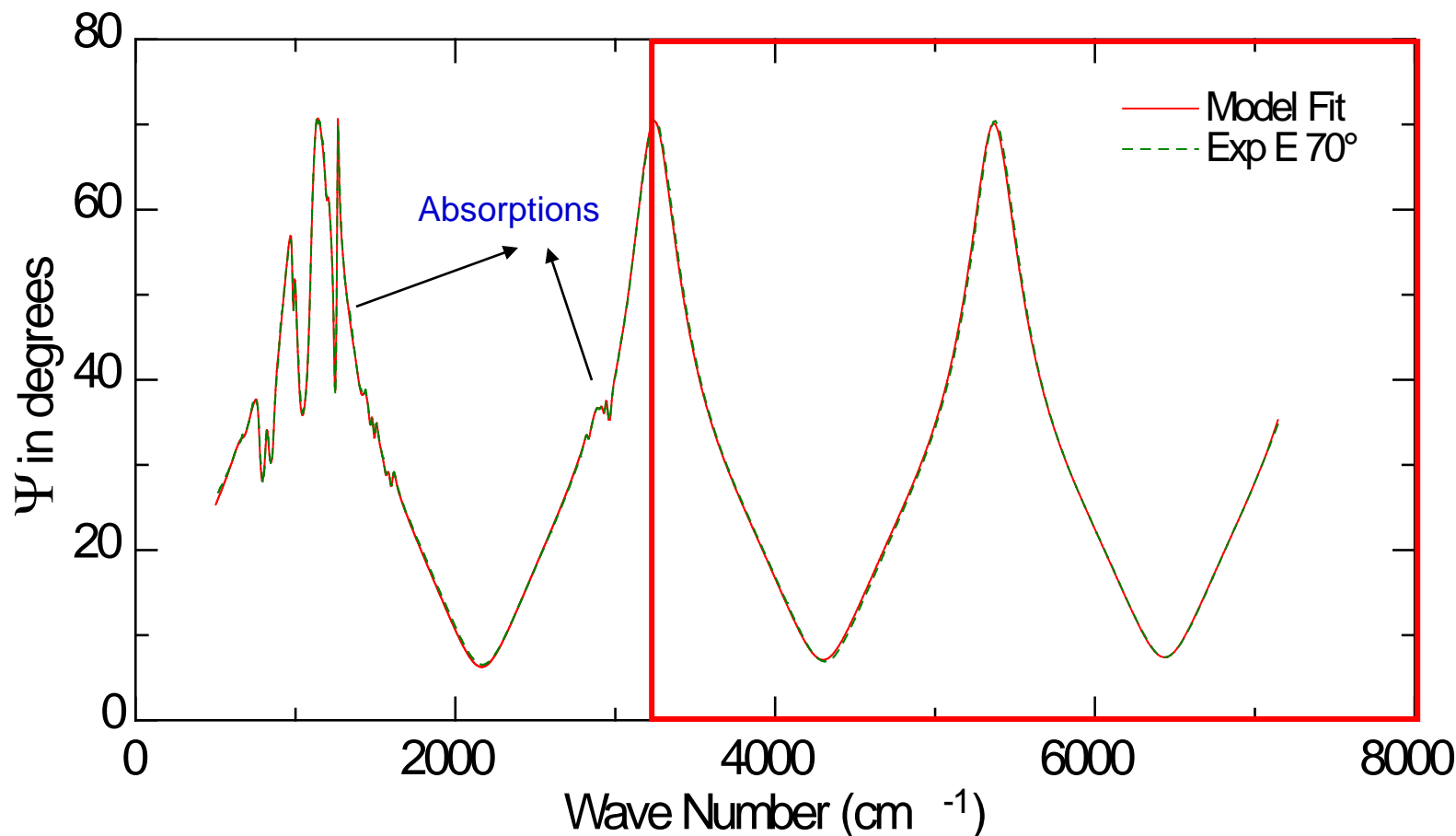
SEM cross-section image

37% cross-linked BCB bond



SAM image

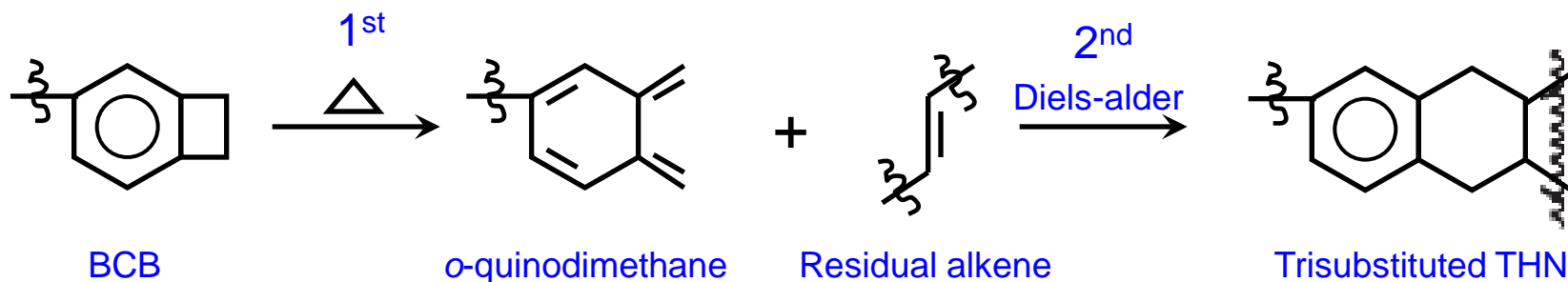
Dendritic structures



$(\Psi, \Delta) \rightarrow (n, t)$ when $k = 0 \Rightarrow$ in a transparent region and determining thickness

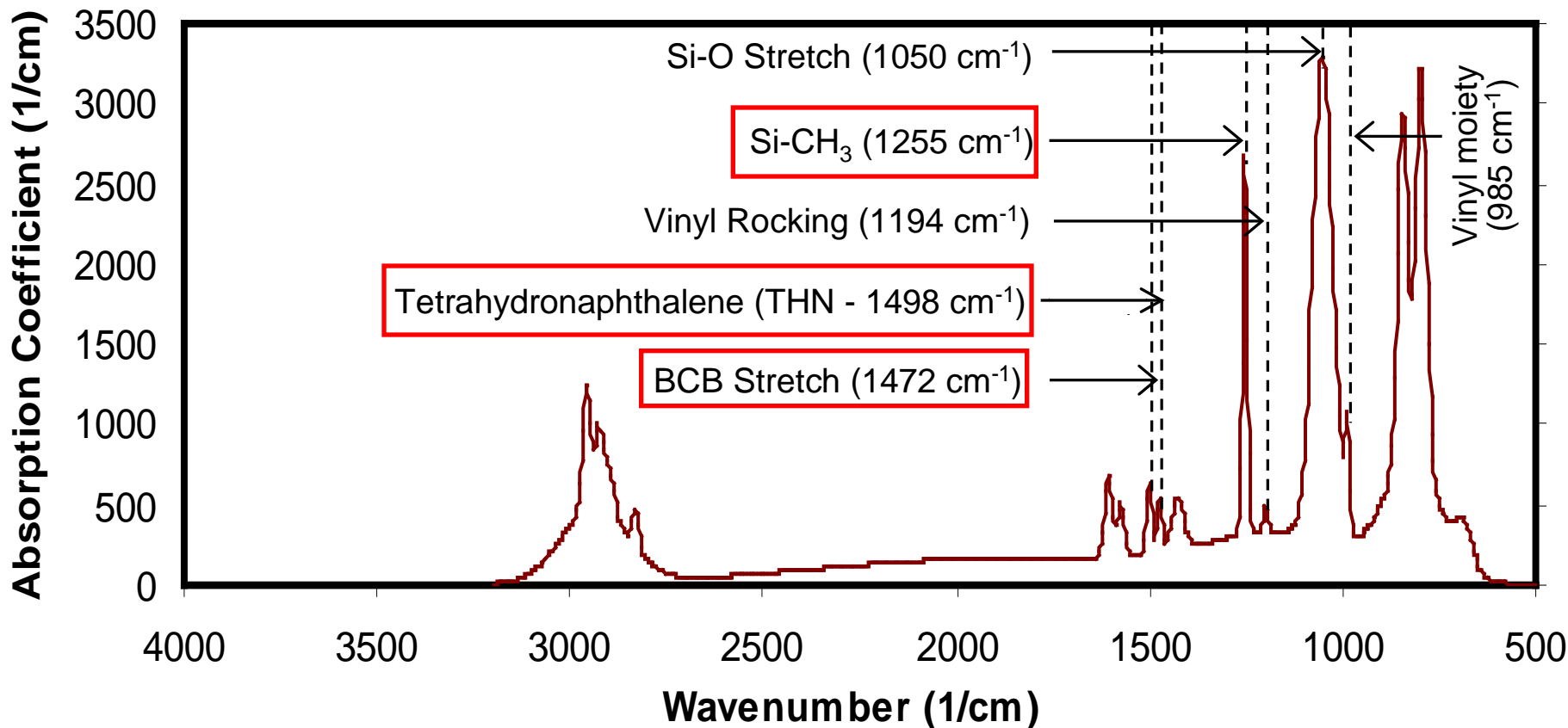
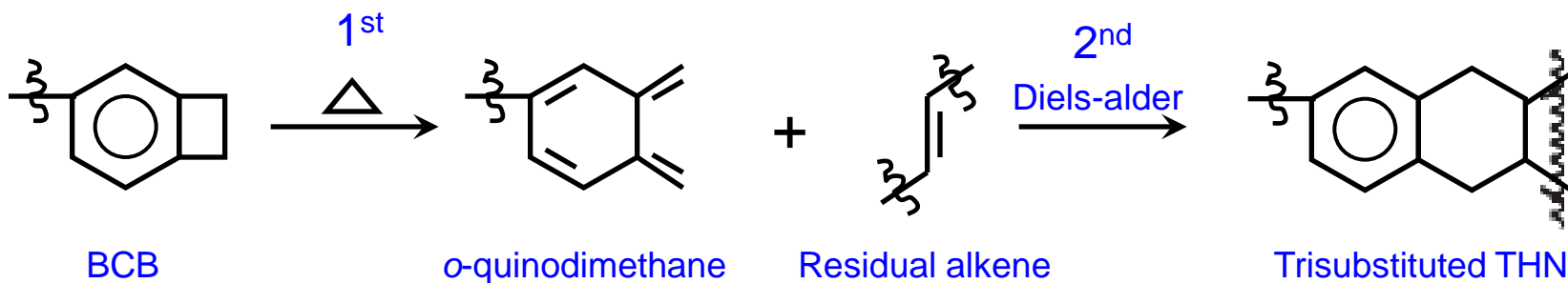
$t \Rightarrow (\Psi, \Delta) \rightarrow (n, k)$ in the entire spectrum

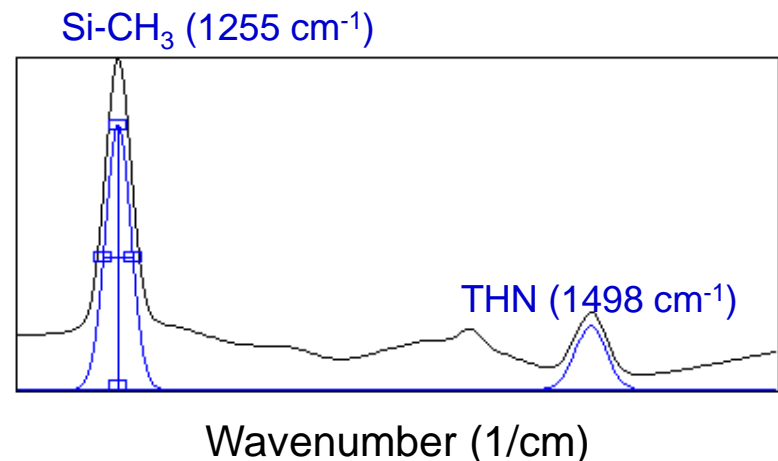
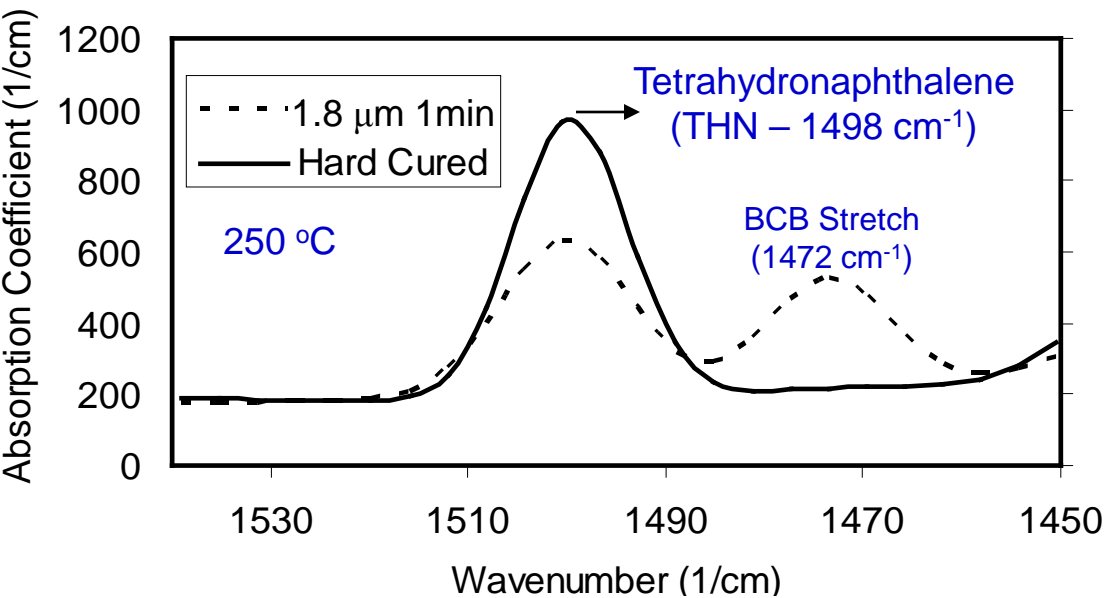




The thermal curing of BCB polymers is a two step process:

1. Thermally activated opening of the BCB ring to form an o-quinodimethane intermediate.
2. The o-quinodimethane reacts with residual alkene groups in the via a Diels-Alder reaction, forming a tri-substituted tetrahydronaphthalene (THN).





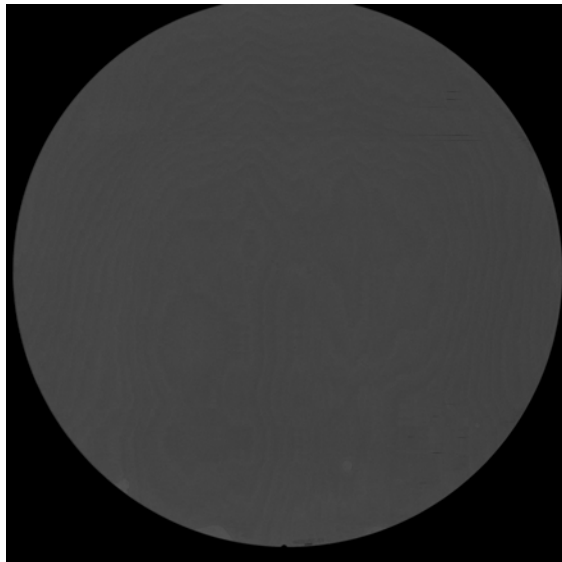
$$\% \text{ curing} = 95 \frac{\left(\frac{A_{1498}}{A_{1255}} \right)_{\text{Film of interest}}}{\left(\frac{A_{1498}}{A_{1255}} \right)_{\text{Hardcured}}}$$

$$\text{Area} = \text{Peak} \times \frac{\text{F.W.H.M}}{\sqrt{2 \ln(2)}} \times \sqrt{2\pi}$$



Hardbake		Cross Linking Level	Experiment Results
Temp °C	Time (min)		
190	10	37%	Dendritic structure and voids were present
190	25	42%	Dendritic structure and voids were present
190	40	45%	Dendritic structure and voids were present
200	15	45%	Dendritic structure and voids were present
200	25	50%	Dendritic structure and voids were present
250	36 (sec)	50%	Dendritic structure and voids were present
200	40	60%	Good no dendrites or voids; passed razor blade test
250	64 (sec)	60%	Good no dendrites or voids; passed razor blade test
250	2	70%	voids were present
250	3.5	80%	No voids were present but failed razor blade test

SAM image

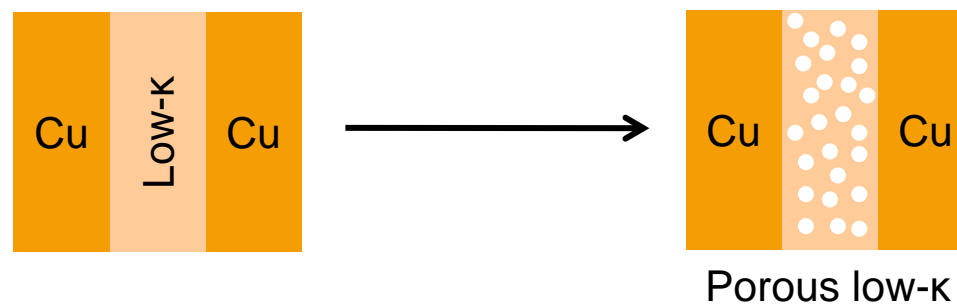


Future Directions:

- Bonding using adhesive materials is relatively new in the semiconductor industry.
 - IRSE can aid in screening newly investigated materials.
 - IRSE will aid in process tuning and development.



Spectroscopic Ellipsometry of Porous Low- κ Dielectric Thin Films



[V.K. Kamineni](#), C.M. Settens, A. Grill, G.A. Antonelli, R.J. Matyi, and A.C. Diebold, *Frontiers of Characterization and Metrology for Nanoelectronics*, AIP Conference Proceedings, 1173 (2009) 168.

C.M. Settens, [V.K. Kamineni](#), G.A. Antonelli, A. Grill, A.C. Diebold, and R.J. Matyi, *Frontiers of Characterization and Metrology for Nanoelectronics*, AIP Conference Proceedings, 1173 (2009) 163.



- Pores reduce the effective dielectric constant of the material
- Decrease signal propagation delays (faster switching speed)
- Reduction in crosstalk and power consumption
- Lower heat dissipation
- Pore volume fraction and pore size will effect the thermo-mechanical properties

IBM (Porous SiCOH)

PECVD of dual-phase materials (matrix and organic precursors)

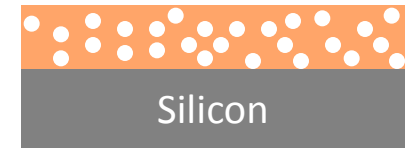
UV cured to desorb porogens (organic precursor)



Sample	κ	Thickness (nm)
SiCOH1	3.0	1000
SiCOH2	2.2-2.4	333
SiCOH3	2.2-2.4	363

Novellus (ULK)

PECVD of porous low- κ with different dielectric constant

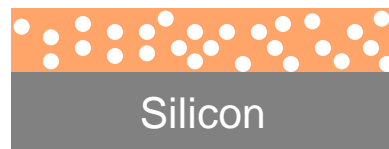
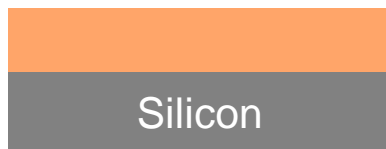


Sample	κ	Thickness (nm)
ULK1	2.75	150
ULK2	2.65	150
ULK3	2.55	150

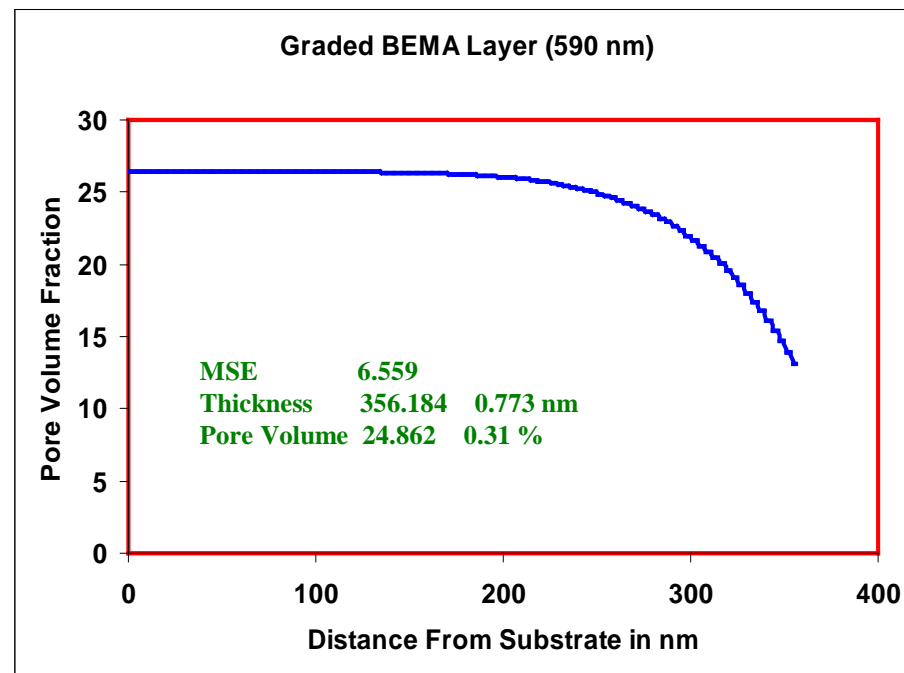
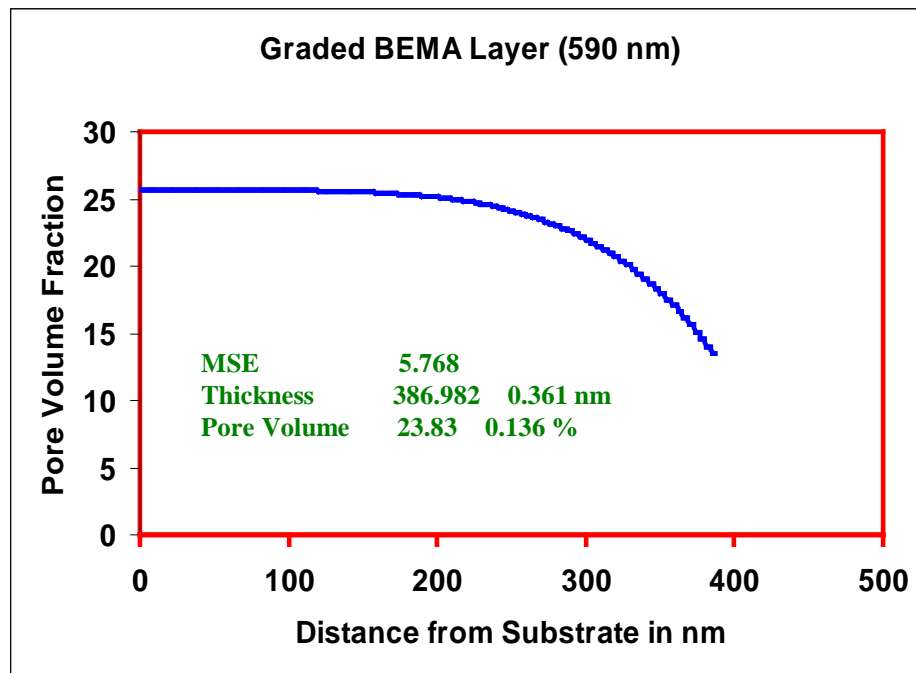


Bruggeman expression for effective medium approximation
on porous SiCOH samples

$$f_a \frac{\epsilon_a - \epsilon}{\epsilon_a + 2\epsilon} + f_b \frac{\epsilon_b - \epsilon}{\epsilon_b + 2\epsilon} = 0$$

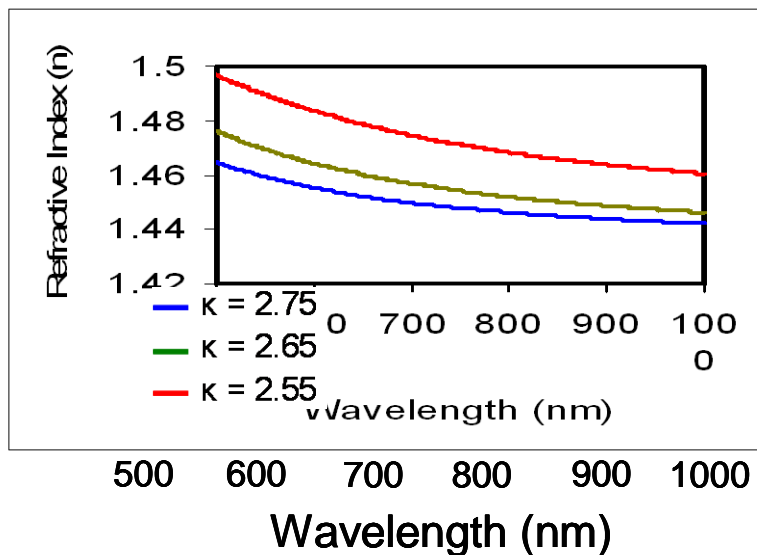


	Pore Volume Fraction	Thickness (nm)
Control	0%	1055.0 0.2
333 nm	24.8 0.3 %	352.6 1.0
363 nm	23.8 0.1 %	379.5 0.4

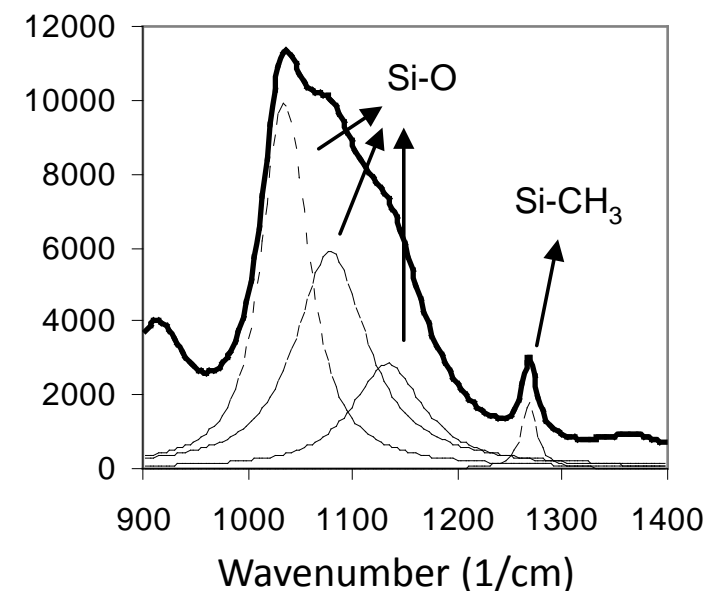




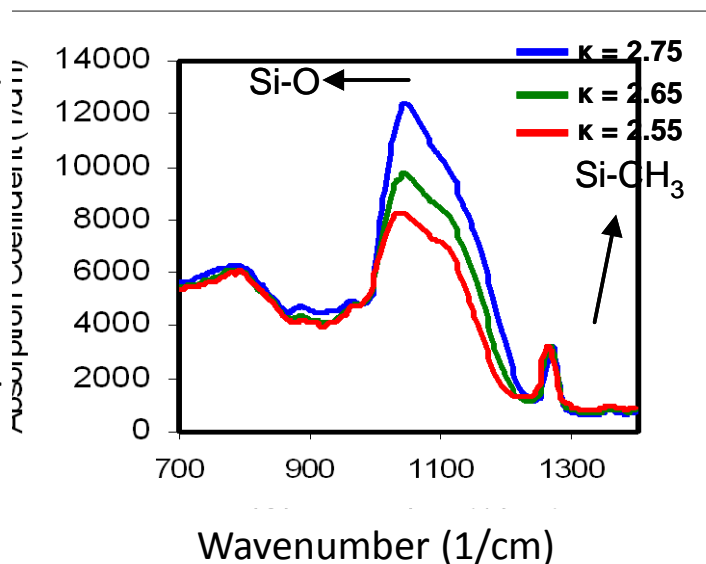
Refractive Index (n)



Absorption Coefficient (1/cm)



Absorption Coefficient (1/cm)

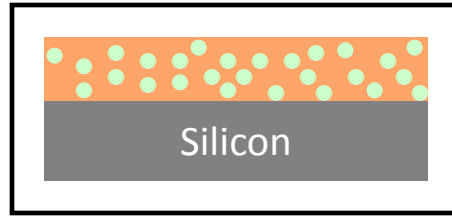


$$\text{Relative Carbon Concentration (\%)} = \frac{A_C}{A_O + A_C}$$

$$\text{Area} = \text{Peak} \times \frac{\text{F.W.H.M}}{\sqrt{2 \ln(2)}} \times \sqrt{2}$$

κ	n	Carbon (%)
2.55	1.48	4
2.65	1.461	2.4
2.75	1.453	1.5

A_C - area under the Si-CH₃ peak
 A_O - area under the Si-O peak



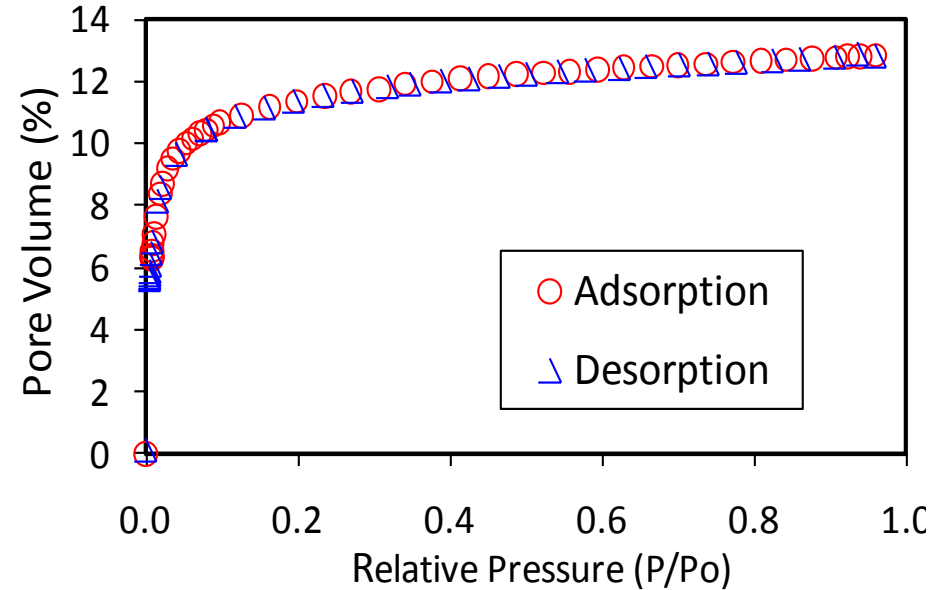
Toluene (low contact angle < 5°)

Lorentz-Lorenz

$$B_{eff} = \frac{3}{4\pi} \cdot \frac{(n_{eff}^2 - 1)}{(n_{eff}^2 + 2)} = \sum N_i \alpha_i$$

$$P = \frac{B_{sat} - B_0}{B_{tol}}$$

$$P = \frac{\frac{n_{sat}^2 - 1}{n_{sat}^2 + 2} - \frac{n_0^2 - 1}{n_0^2 + 2}}{\frac{n_{tol}^2 - 1}{n_{tol}^2 + 2}}$$



B_{eff} – effective polarizability

n_{eff} – effective refractive index (RI)

N_i - number of molecules

α_i – molecular polarizability

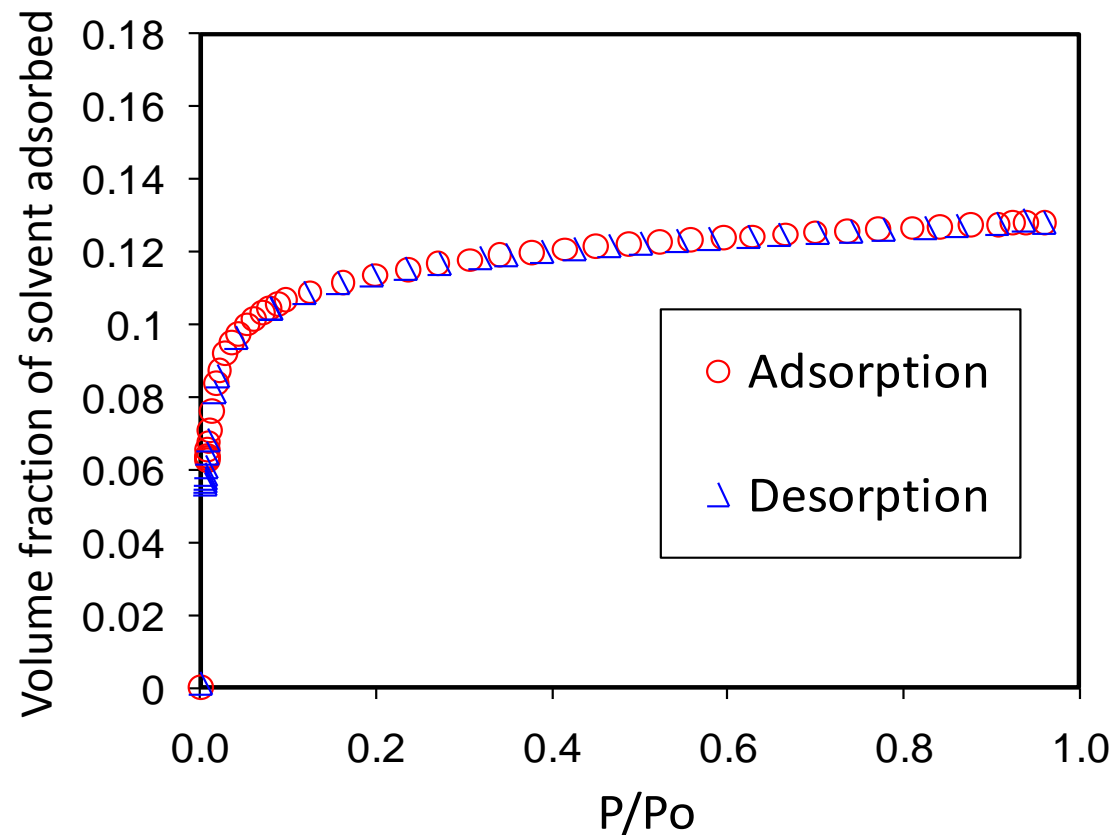
n_{sat} – RI of film filled with toluene

n_{tol} – RI of toluene

n_0 – RI of film without toluene

P - porosity

Sample	Refractive Index (n)	Porosity (%)
$\kappa = 2.55$	1.48	13.19
$\kappa = 2.65$	1.461	11.76
$\kappa = 2.75$	1.453	7.92



Dubinin and Radushkevitch (DR)

$$V = V_0 \exp \left[-\frac{1}{(\beta E_0)^2} \left(RT \ln \frac{P}{P_0} \right)^2 \right]$$

$$\ln V = \ln V_0 - BA^2$$

$$A = RT \ln \left(\frac{P_0}{P} \right) \quad B = \frac{1}{(\beta E_0)^2}$$

$$r = \frac{K}{2E_0}$$

A – adsorption potential

R – universal gas constant

V – adsorbate volume

V_0 – total micro pore volume

β – function of toluene only

E_0 – solid characteristic energy towards a reference adsorbate

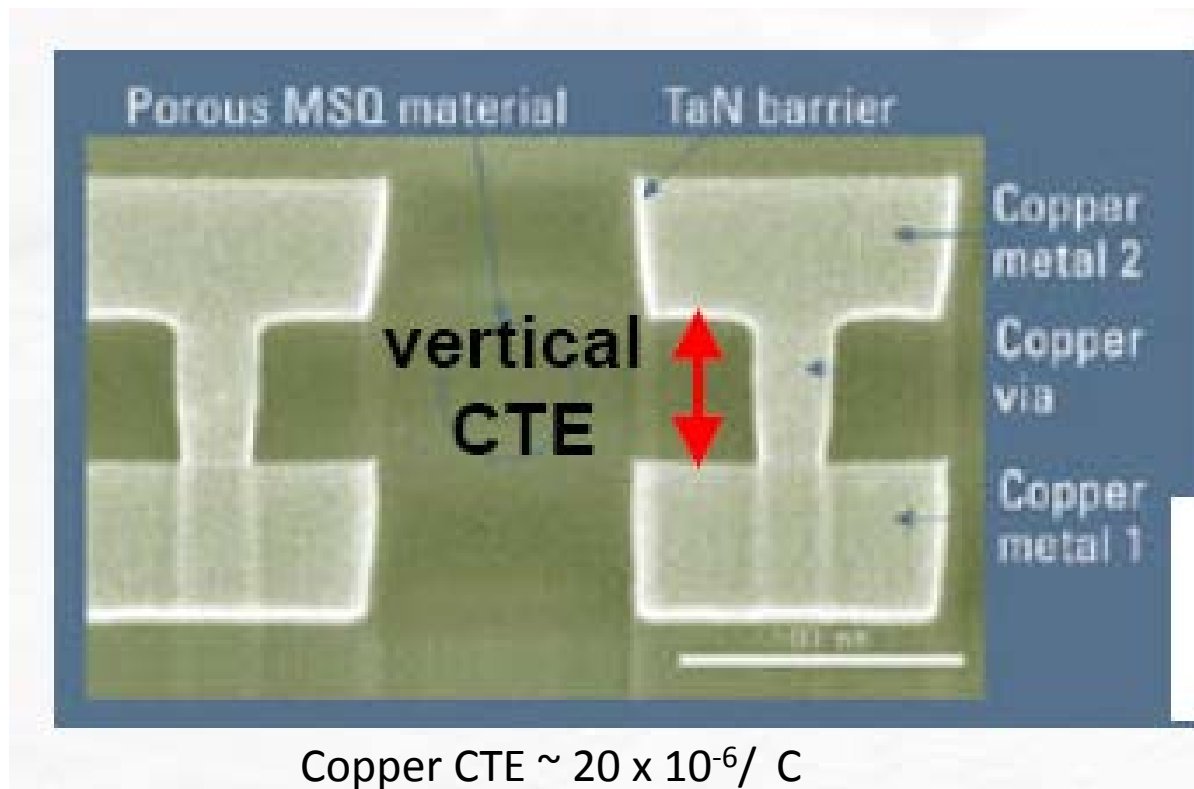
K – empirical constant ≈ 12

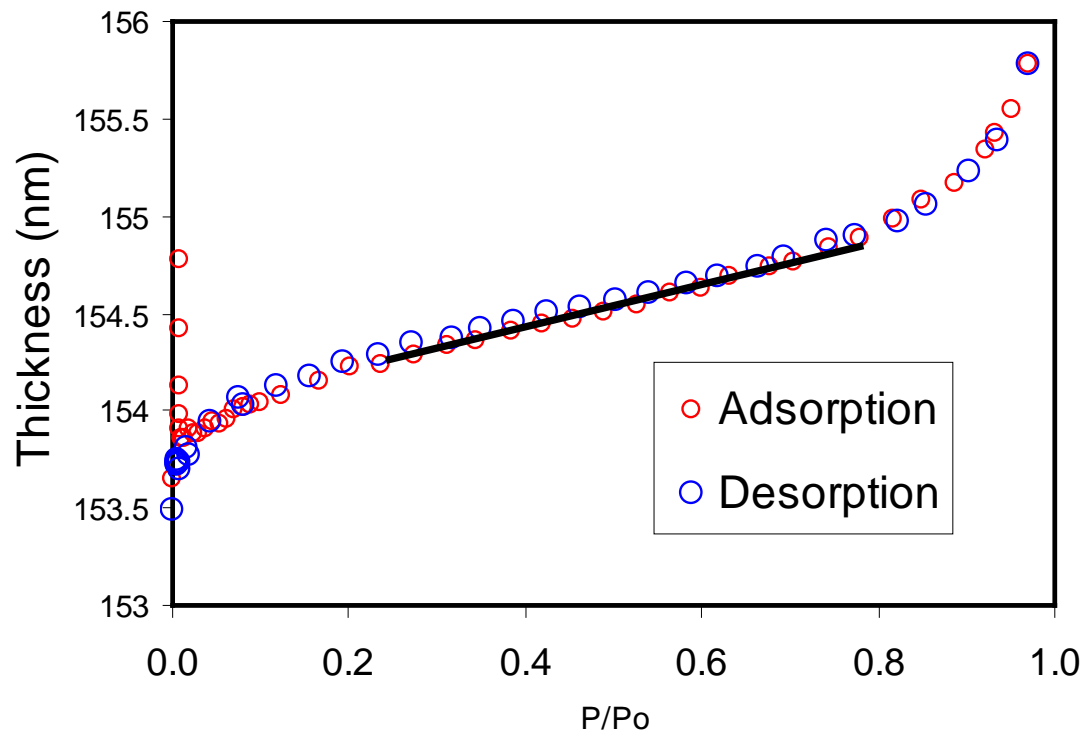
Sample	Refractive Index (n)	Pore radius (nm)
$\kappa = 2.55$	1.48	0.82
$\kappa = 2.65$	1.461	0.79
$\kappa = 2.75$	1.453	0.84



SE can measure critical mechanical parameters (Young's modulus, CTE)

- Young's modulus is a measure of the stiffness of the porous low- κ dielectric material
- A low CTE will prevent a connection failure between via/M1 and/or via/M2





K. P. Mogilnikov and M. R. Baklanovz

$$d = d_0 - k \ln \frac{P}{P_0}$$

$$E = \frac{d_0 RT}{k V_L}$$

Sample	Porosity (%)	Pore radius (nm)	EP Young's Modulus (GPa)
$\kappa = 2.55$	13.19	0.82	2.74
$\kappa = 2.65$	11.76	0.79	3.96
$\kappa = 2.75$	7.92	0.84	7.08

V_L – molecular volume

E – Young's modulus



Free standing film (thermal expansion rate)

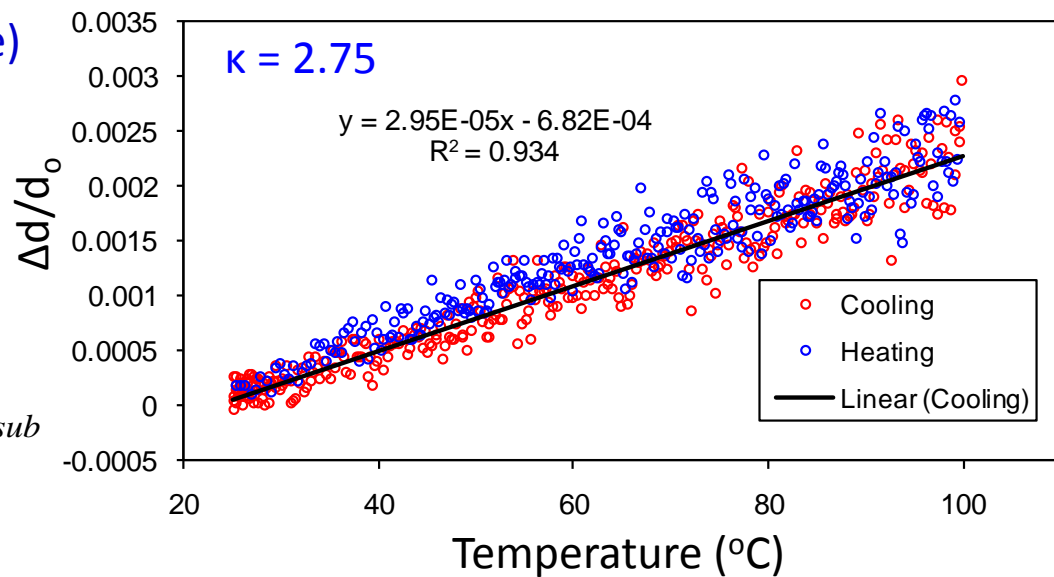
$$\frac{1}{L_o} \frac{dL}{dT} = \alpha$$

Film on substrate (CTE)

$$\frac{1}{L_o} \frac{dL}{dT} = \left(\frac{1 + \nu_{film}}{1 - \nu_{film}} \right) \alpha_{film} - \left(\frac{2\nu_{film}}{1 - \nu_{film}} \right) \alpha_{sub}$$

ν_{film} = Poisson's Ratio = 0.25

$\alpha_{substrate} = 2.6 \times 10^{-6} / ^\circ C$



$$\frac{1}{L_o} \frac{dL}{dT} = \alpha = 29.5 \times 10^{-6} / ^\circ C$$

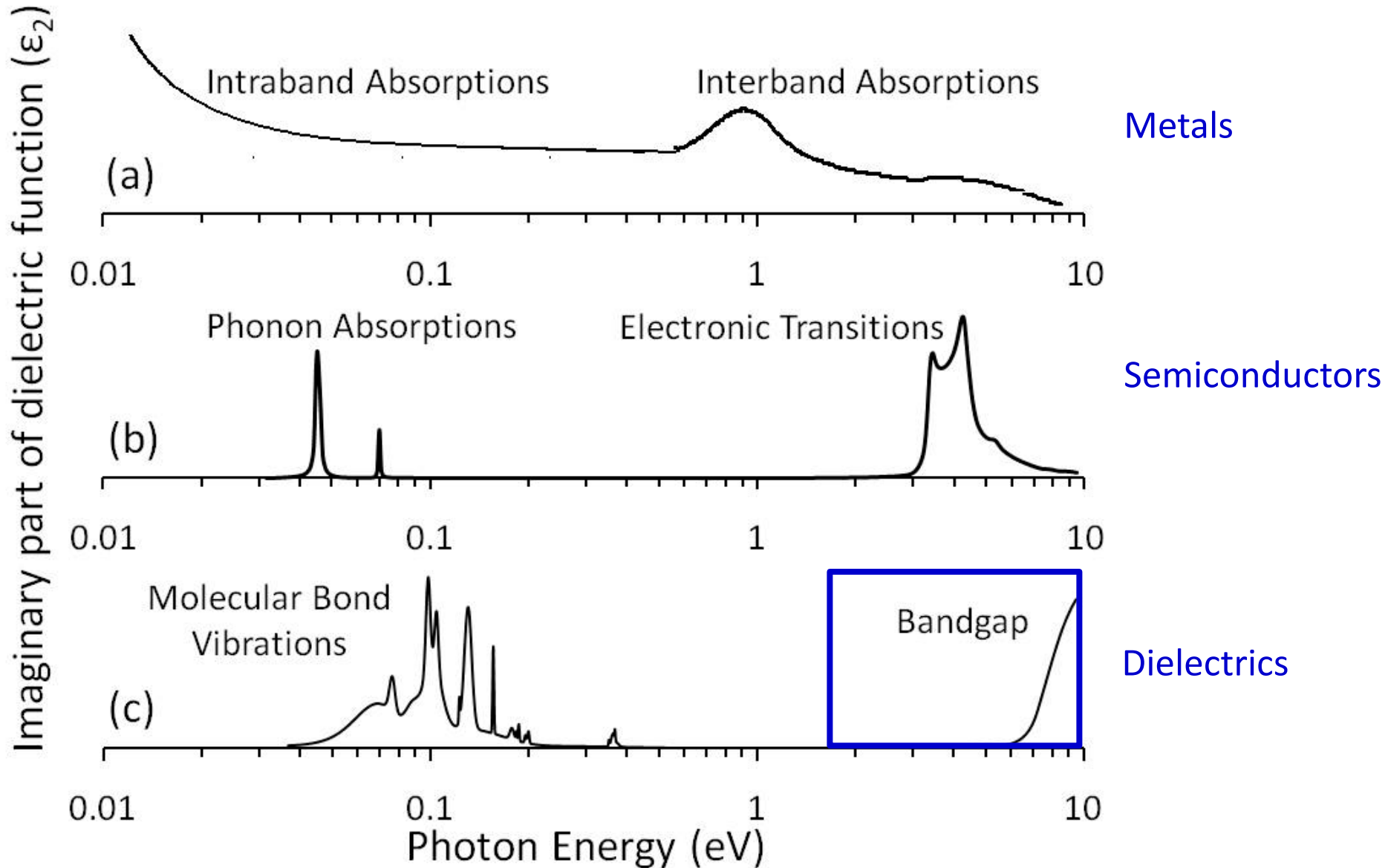
Sample	Refractive Index (n) 632.8 nm	TER (10 ⁻⁶ /°C)	CTE (10 ⁻⁶ /°C)
κ = 2.55	1.48	70.2	44.72
κ = 2.65	1.461	54.9	35.54
κ = 2.75	1.453	29.5	20.30

Note: Fitting for the substrate expansion using the silicon temperature library (J.A.Woollam)



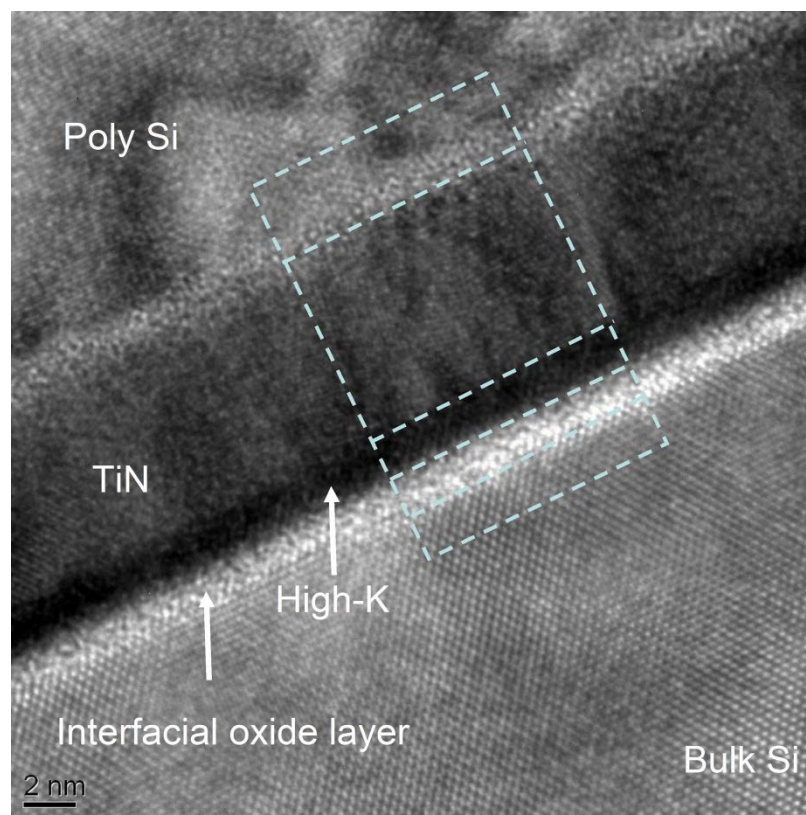
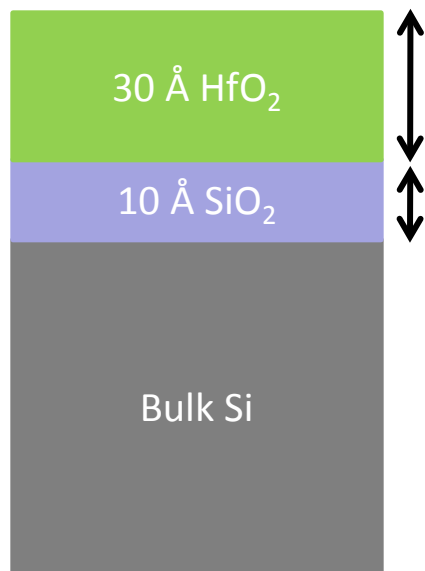
- The following parameters were determined using SE.
 - SICOH (IBM)
 - Porosity (BEMA)
 - Grading in porosity
 - ULK (Novellus)
 - Carbon content
 - Porosity (EP)
 - Pore size
 - Young's modulus
 - Coefficient of thermal expansion
- Complementary techniques such as specular XRR, off-specular XRR and SAXS were also performed on these films. Both, the optical and x-ray metrology agreed reasonably well.

Sample	Thickness (nm)	n (632.8 nm)	Carbon %	Porosity (%)	Pore radius (nm)	EP Young's Modulus (GPa)	TER ($10^{-6}/^{\circ}\text{C}$)	CTE ($10^{-6}/^{\circ}\text{C}$)
$\kappa = 2.55$	155.6	1.48	4	13.19	0.82	2.74	70.2	44.72
$\kappa = 2.65$	154.7	1.461	2.4	11.76	0.79	3.96	54.9	35.54
$\kappa = 2.75$	147.1	1.453	1.5	7.92	0.84	7.08	29.5	20.30

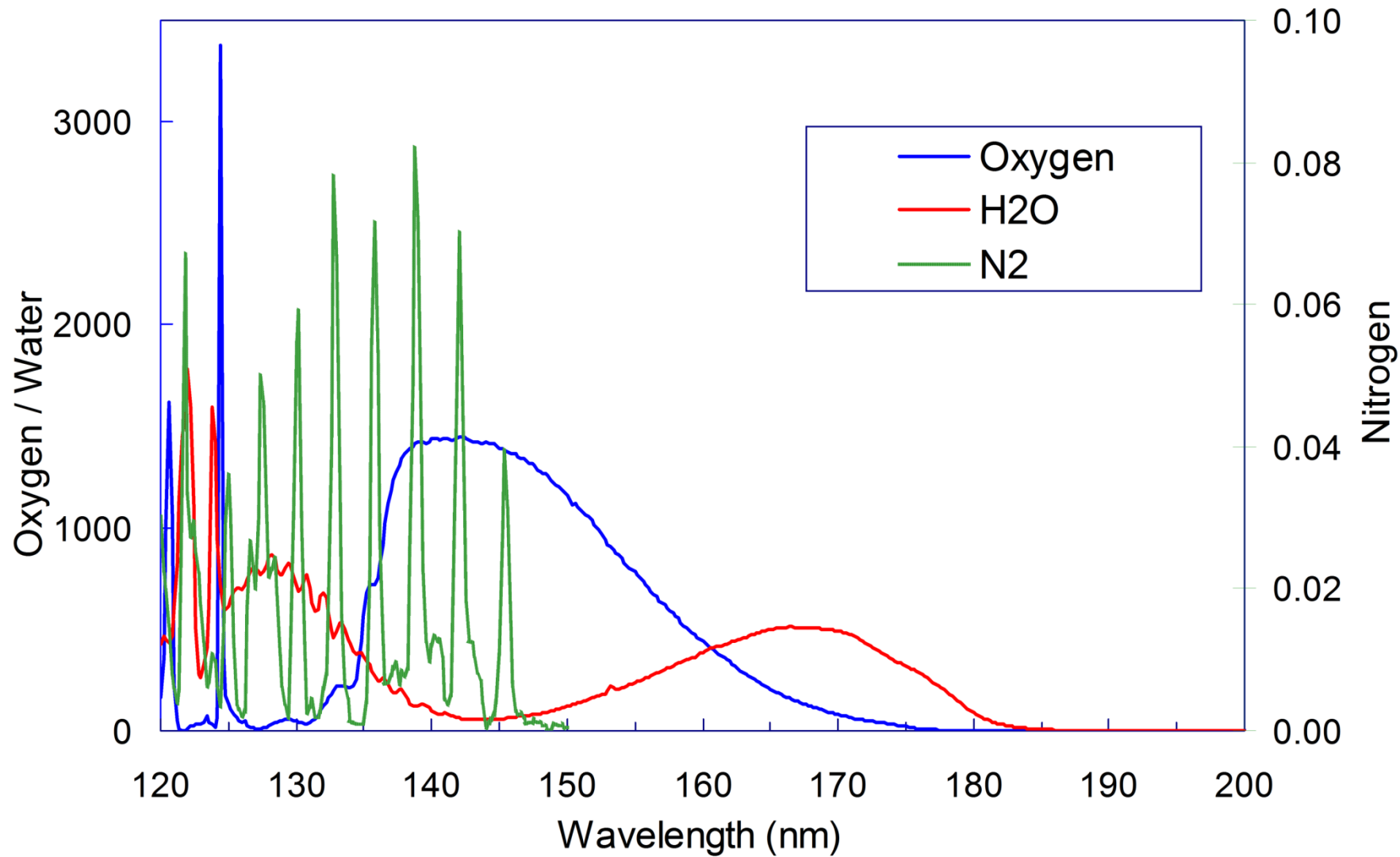




Extension of Far UV spectroscopic ellipsometry studies of High-κ dielectric films to 130 nm



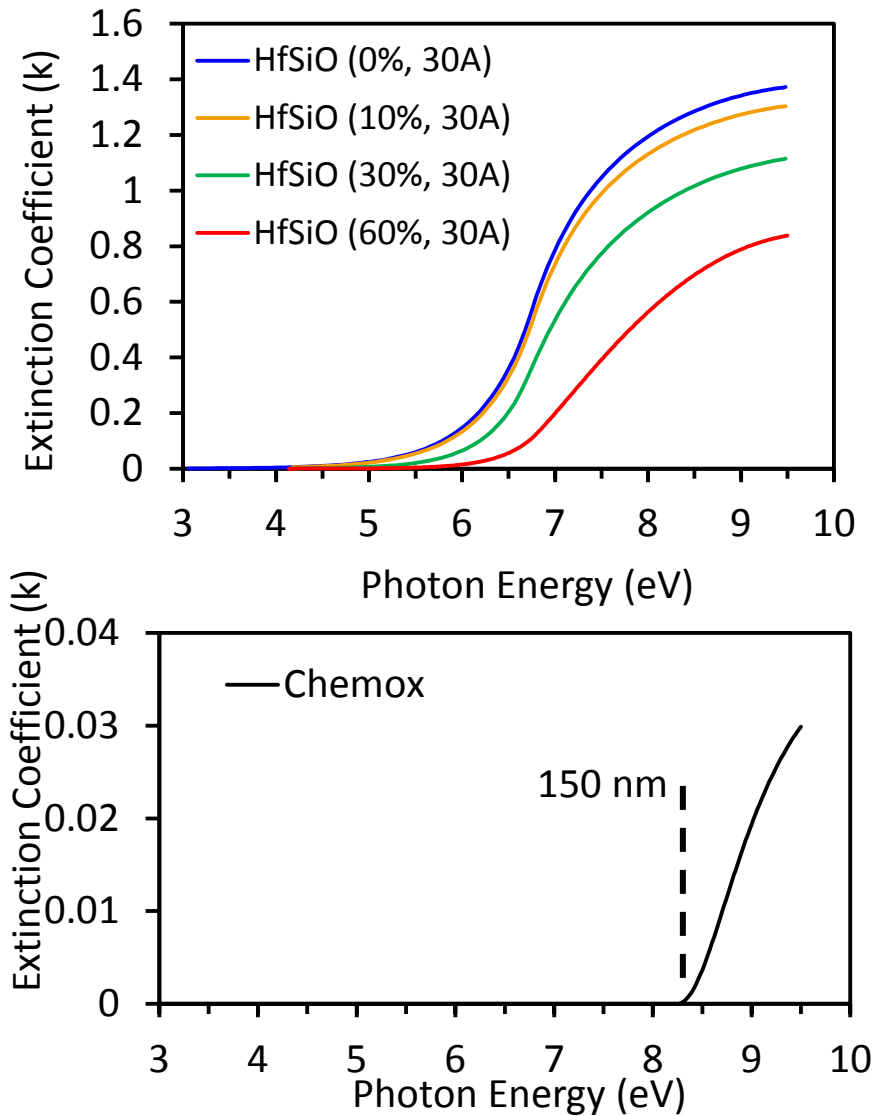
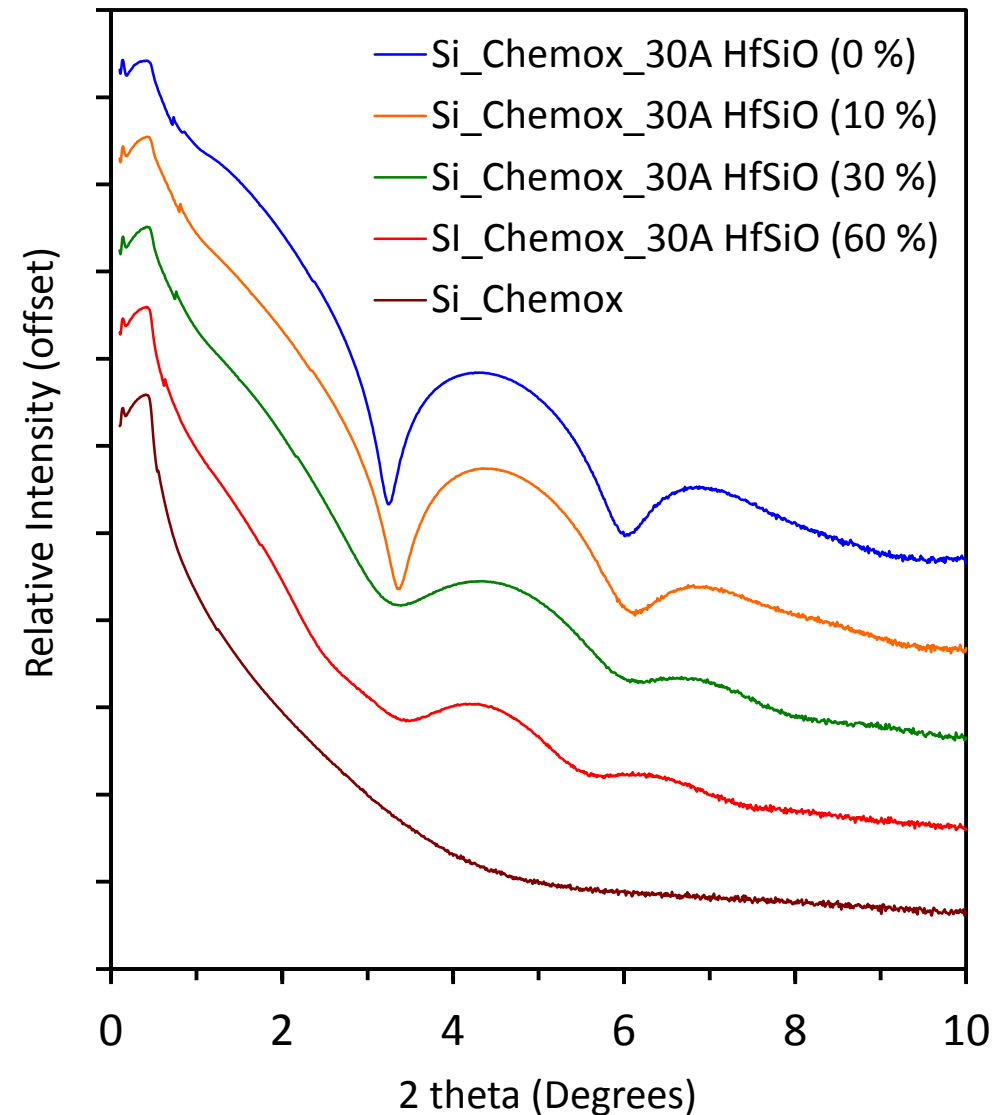
V. K. Kamineni, J. Hilfiker, J. Freeouf, S. Consiglio, R. Clark, G.J. Leusink, and A. C. Diebold, *Thin Solid Films*, 519 (2011) 2894.

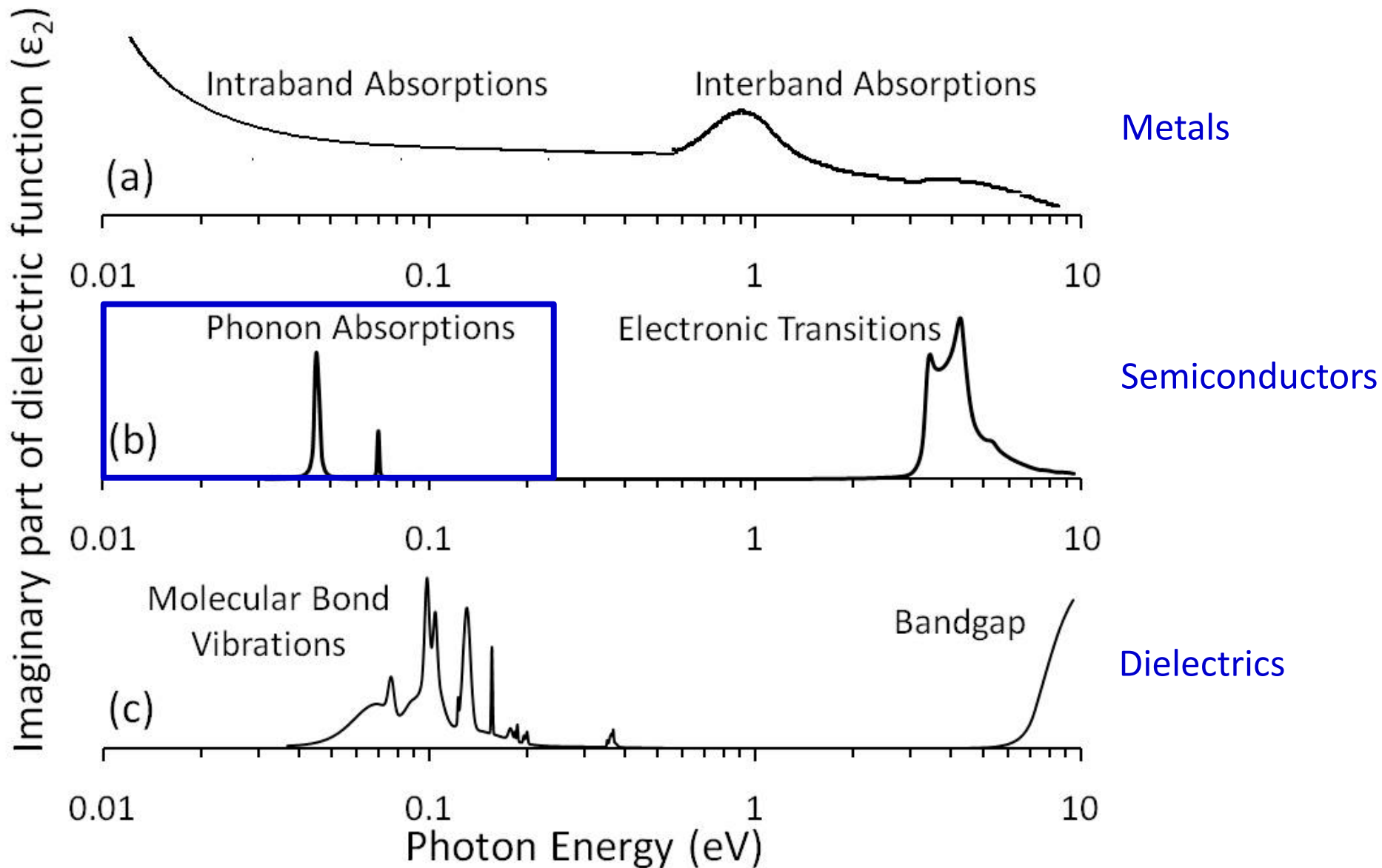




XRR

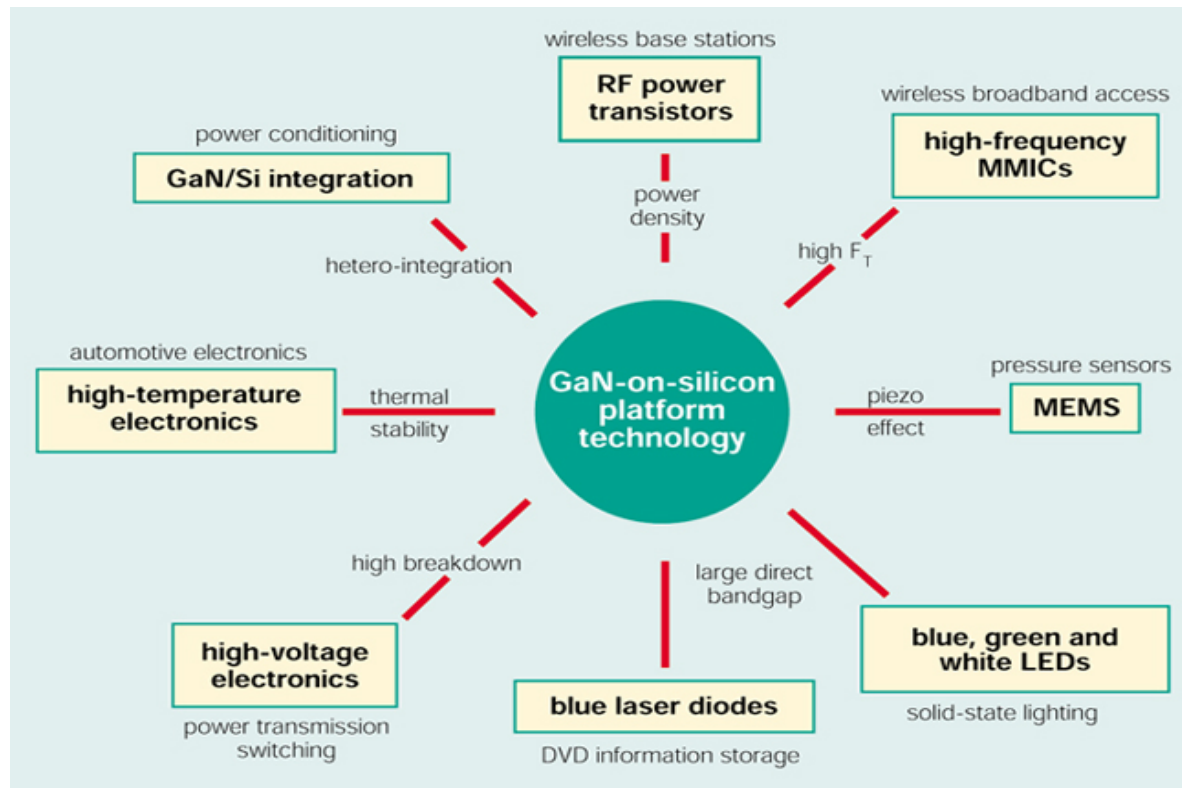
SE







Metrology of Strain Engineered GaN/AlN/Si(111) Thin Films Grown by MOCVD

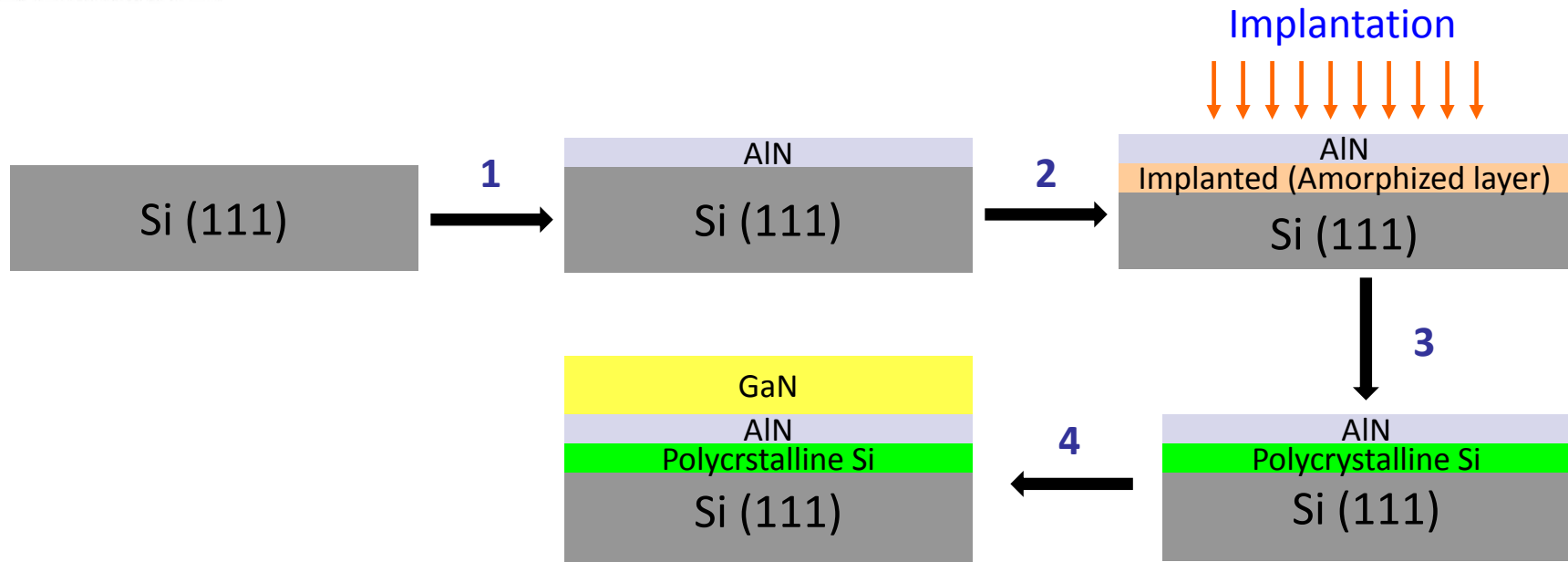


M. Tungare, V. K. Kamineni, F. Shahedipour-Sandvik and A. C. Diebold, Thin Solid Films, 519 (2011) 2929.



Wide Band Gap Optronix Lab

Prof. Shadi Shahedipour-Sandvik and Mihir Tungare

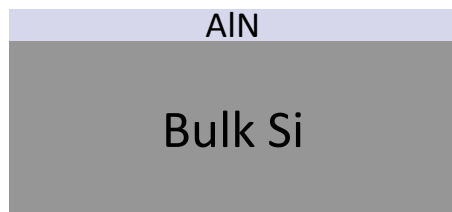


Substrate engineering consists of 4 major steps:

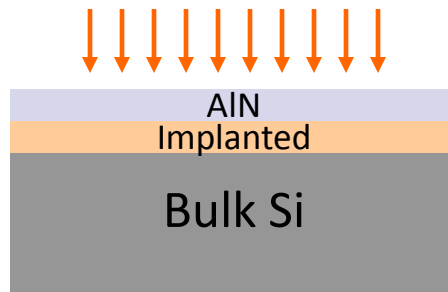
- 1) Growth of an epitaxial AlN buffer layer on Si
- 2) Implantation of AlN/Si with N⁺ ions to create a defective layer in Si below AlN buffer
- 3) Annealing of AlN/Si to recover any loss of crystallinity due to implantation
- 4) Growth of thick (2 μm) GaN on AlN/Si



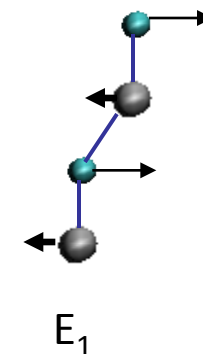
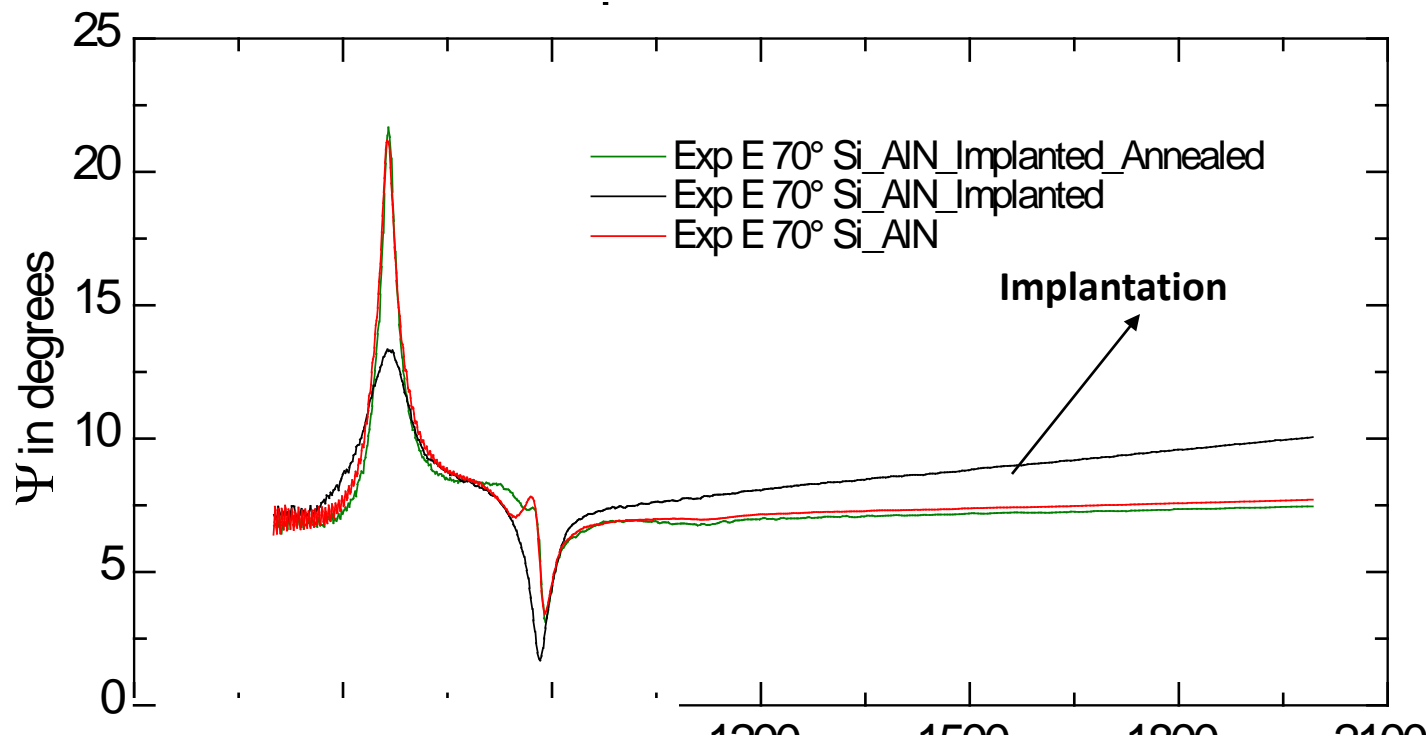
(1) AlN/Si



(2) Implanted (60 keV N¹⁴⁺)



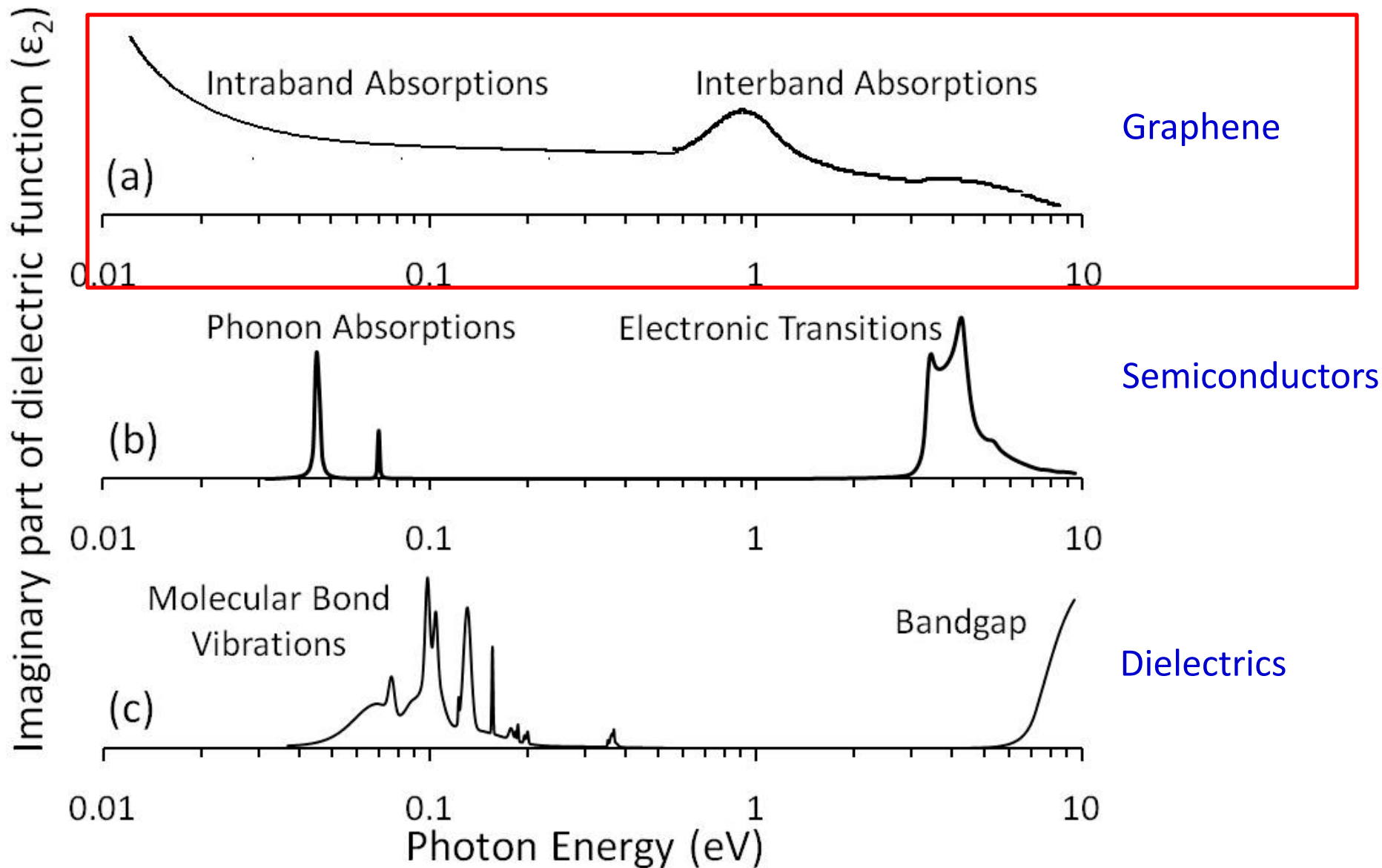
(3) Annealed (1100 °C)

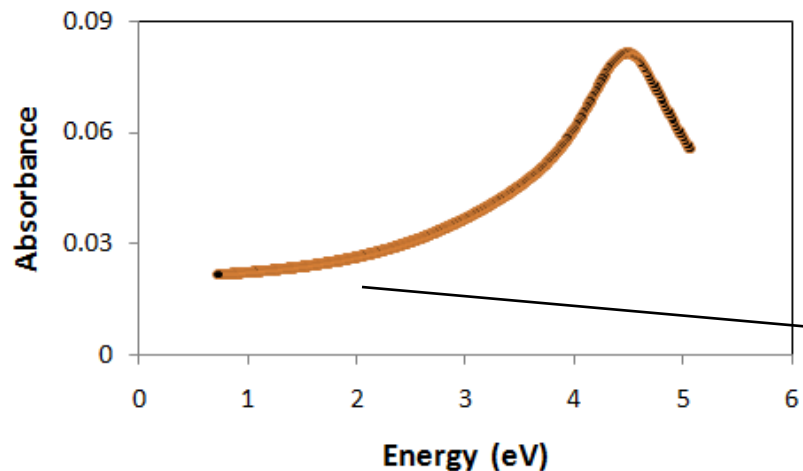
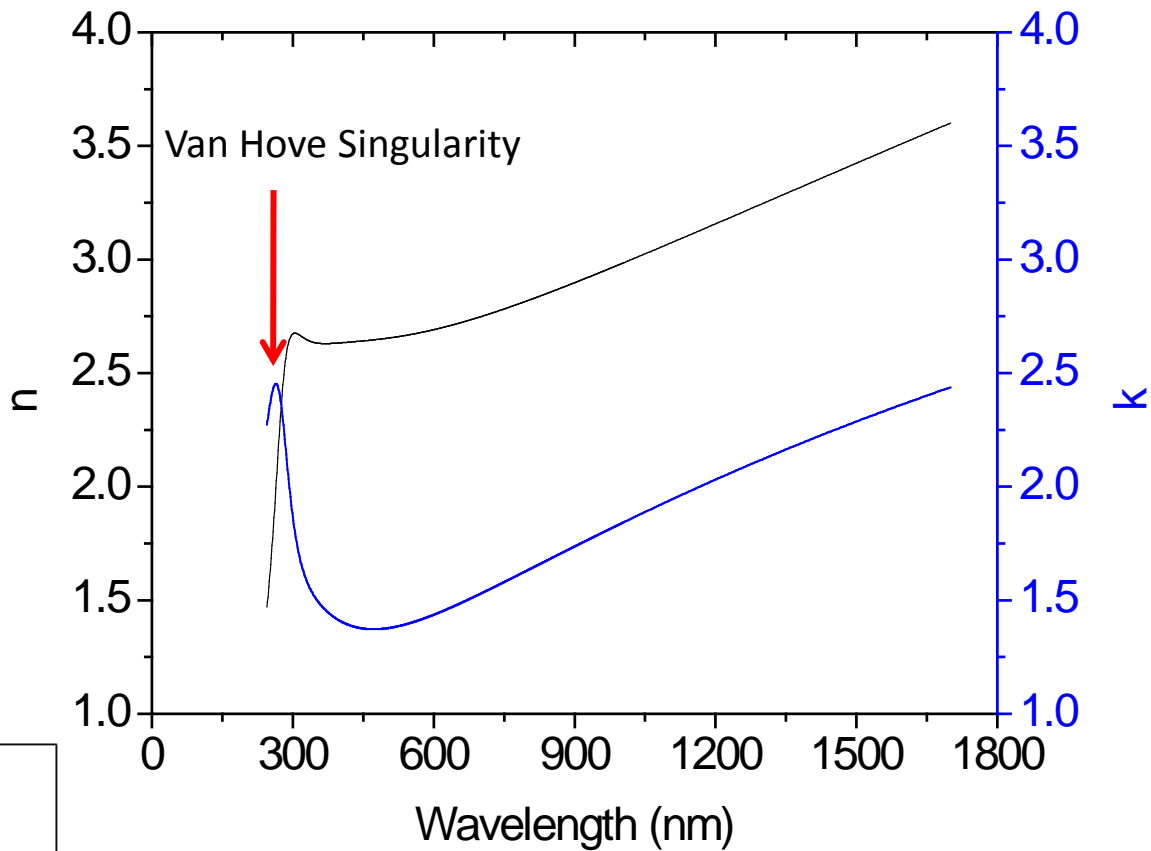
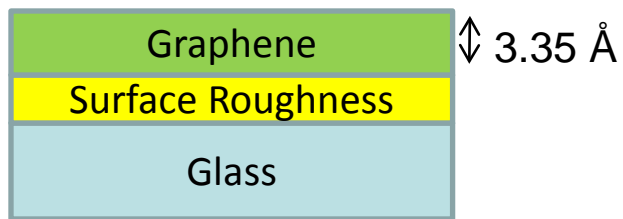




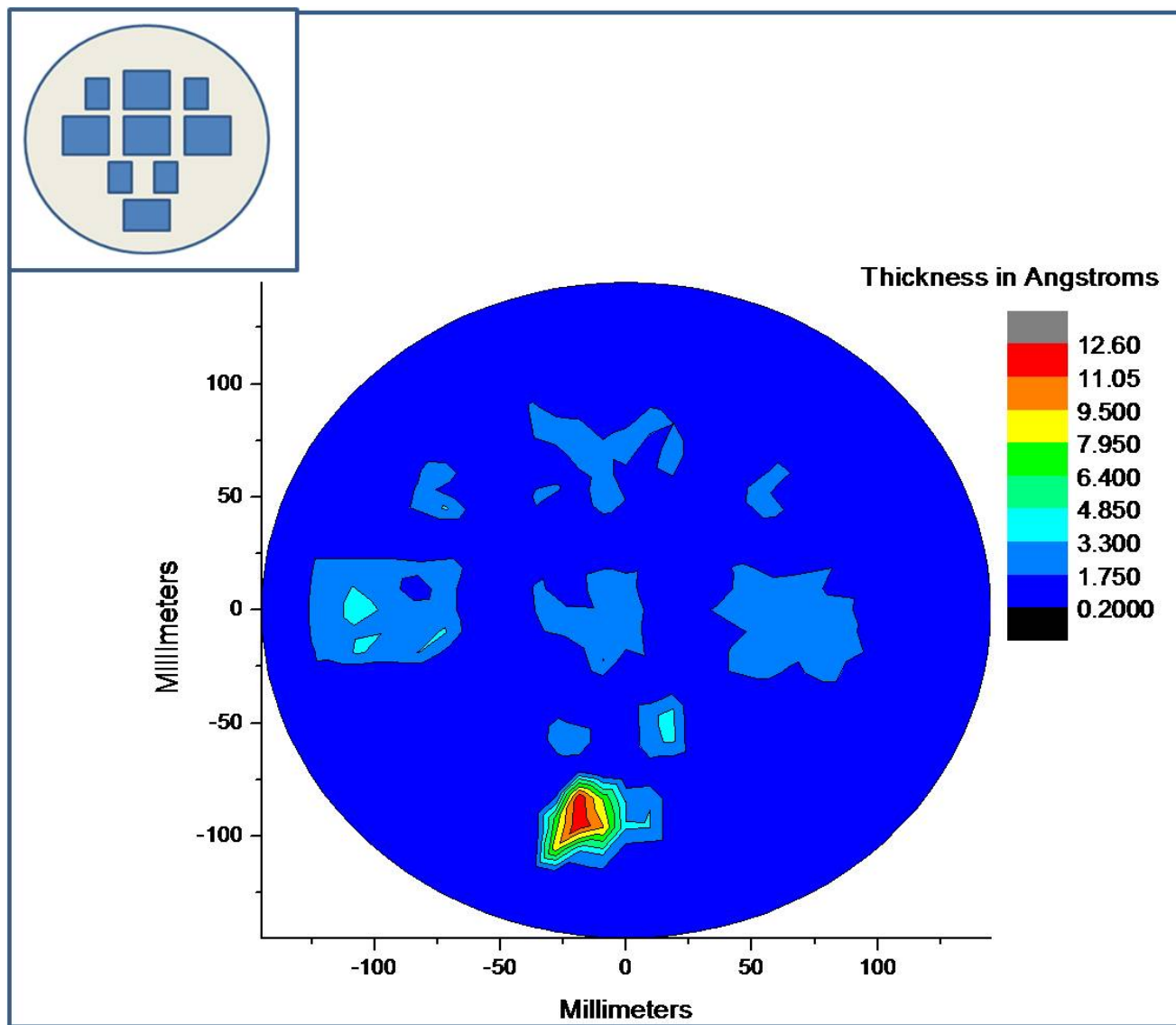
- Resolution = 2 cm^{-1}
- E_1 (TO) Bulk AlN = 666 cm^{-1}
- Isotropic model due to very thin AlN films (IR Probe)
- Tensile Biaxial Strain
- Broadening of the E_1 (TO) phonon mode in implanted AlN is clear sign of presence of defects
- Not sensitive to the A_1 (TO) due to c-plane orientation

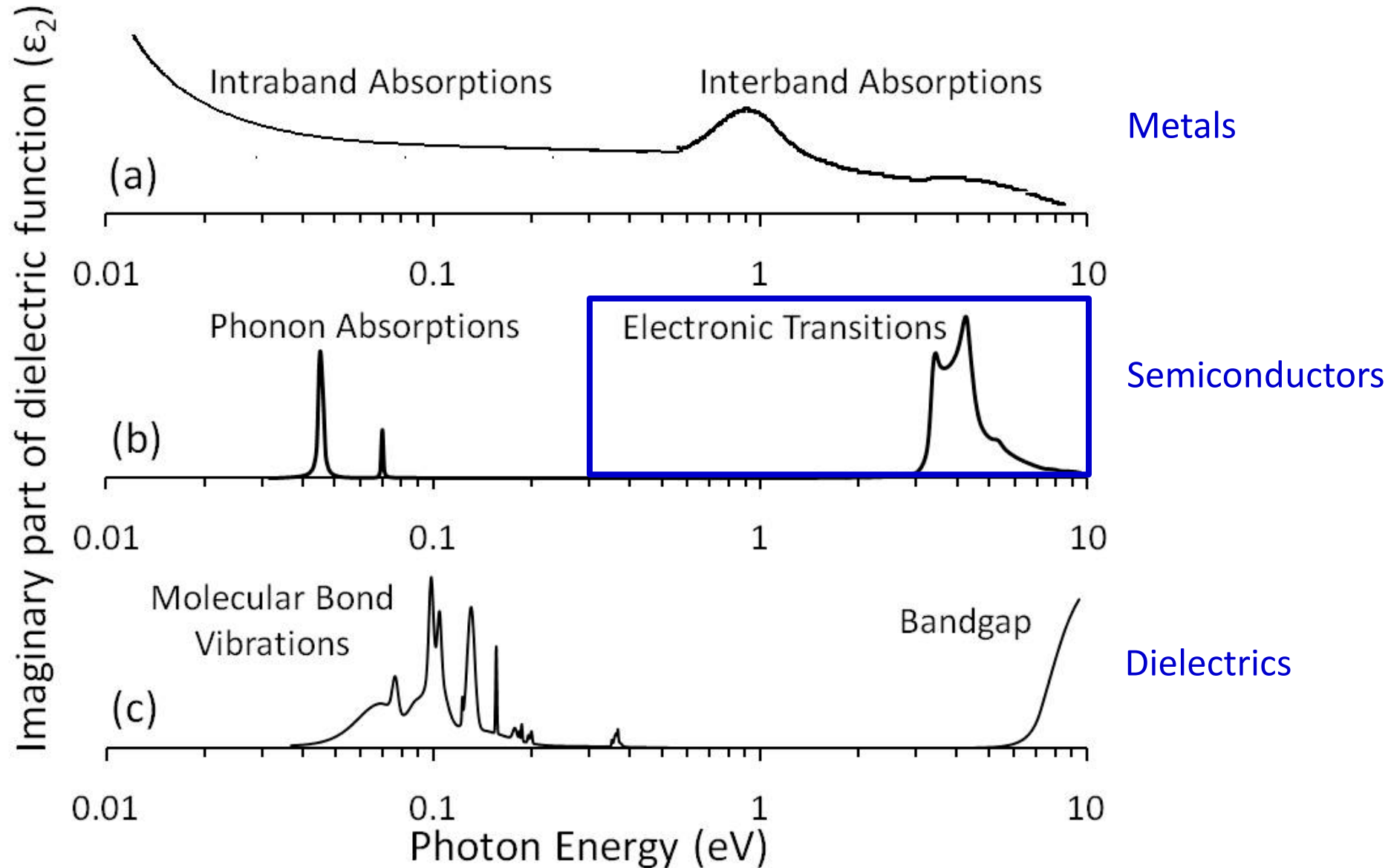
Sample List	$E_1(\text{TO}) \text{ cm}^{-1}$	$\gamma \text{ (cm}^{-1}\text{)}$	$\Delta\omega \text{ (cm}^{-1}\text{)}$	$d\omega_o/dP$	Stress (GPa)
Si_AIN	662.2 0.08	19.5 0.2	3.8	4.5	0.84
Si_AIN_Implanted	664.5 0.24	56.0 0.4	1.5	4.5	0.33
Si_AIN_Annealed	663.8 0.16	21.2 0.2	2.1	4.5	0.48





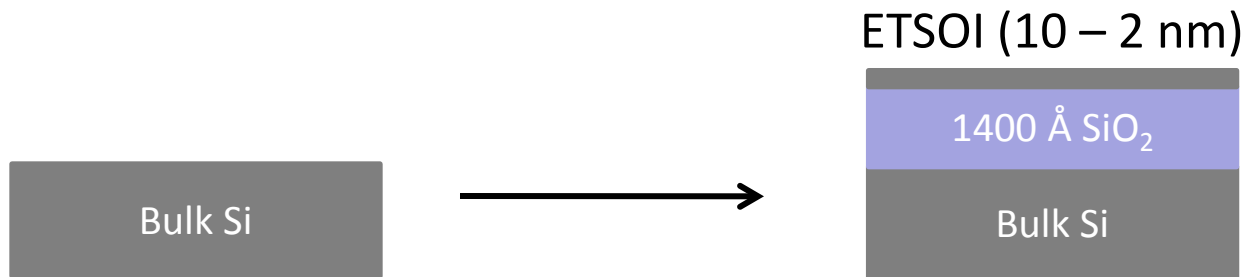
*Graphene's infrared-to-visible absorbance: $\sim 2.3\%$





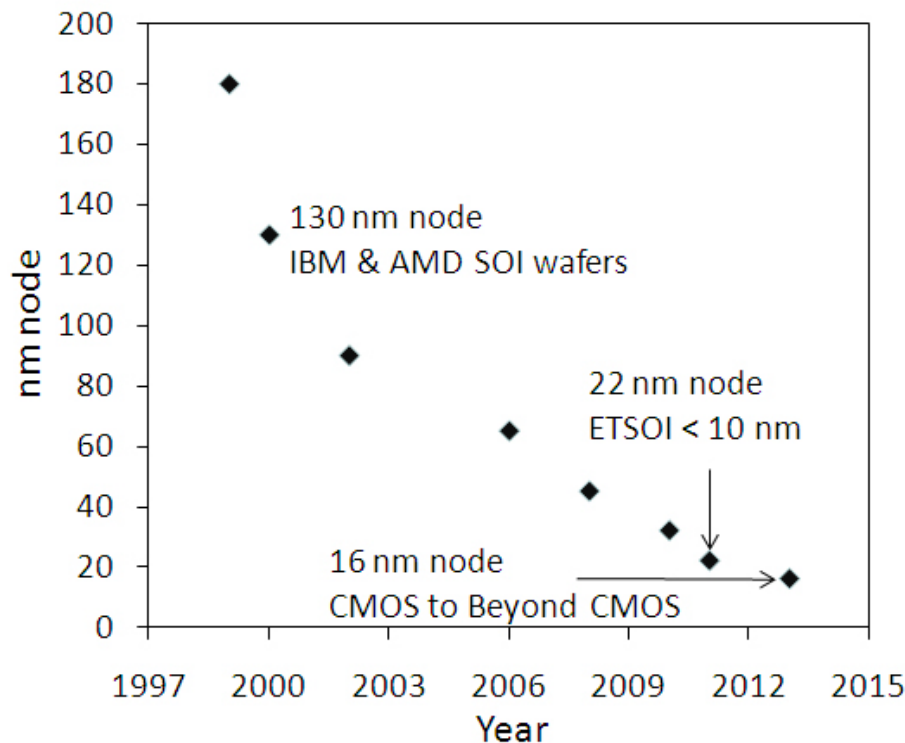
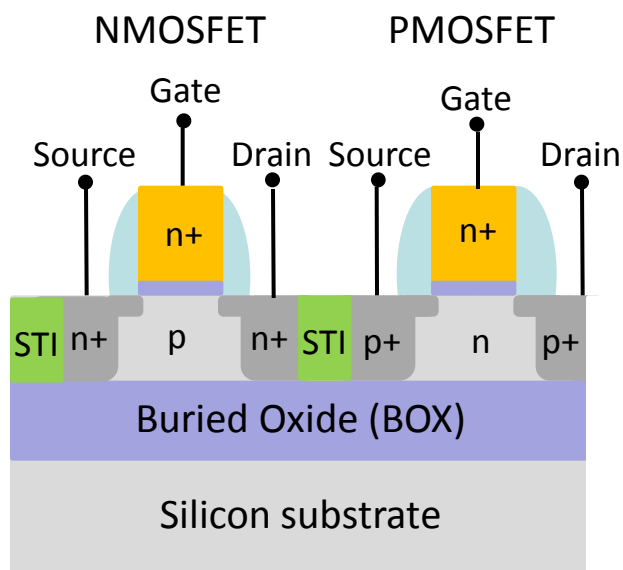


Temperature and thickness dependence of the dielectric function and interband critical points in ETSOI



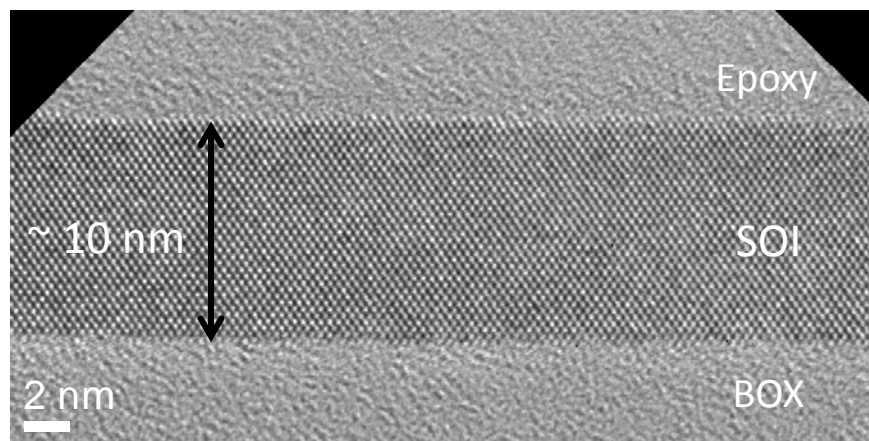
Dielectric response of bulk Si and nanoscale silicon films in different

V. K. Kamineni and A. C. Diebold, "Evidence of the phonon confinement on the linear optical response of nanoscale silicon films", [arXiv:1103.4102v2](https://arxiv.org/abs/1103.4102v2).



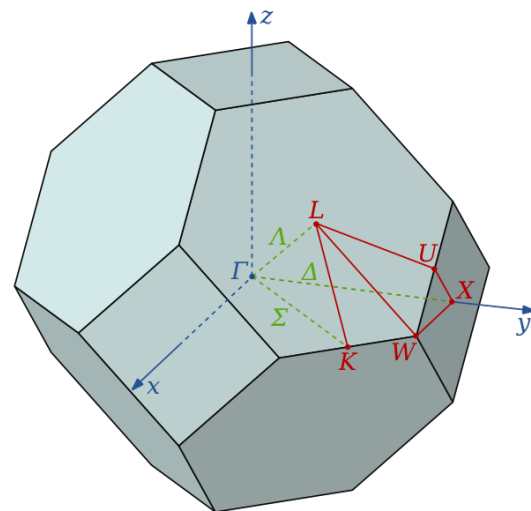
Advantages of SOI technology:

- Excellent isolation of active devices
- Lowers the parasitic capacitance
- Lower leakage current
- Faster device operation
- Lower power consumption





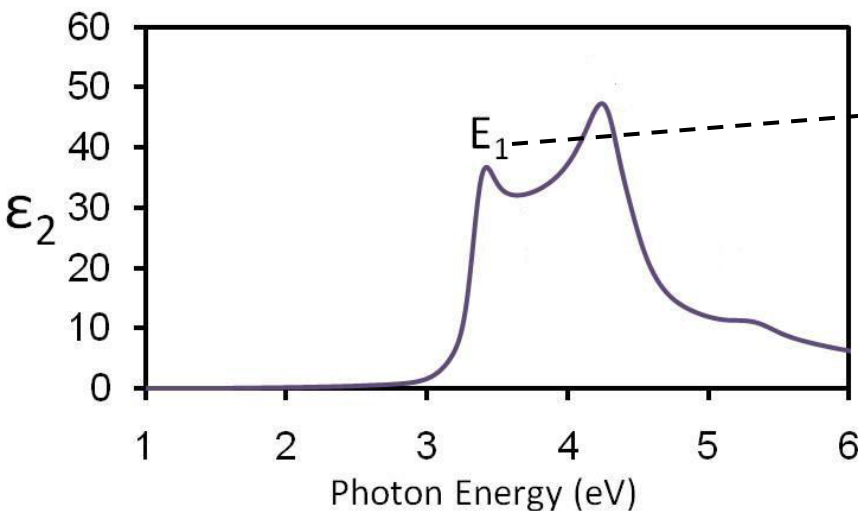
First Brillouin zone (truncated octahedron) of FCC Lattice¹



[100] Direction: Γ Δ X

[111] Direction: Γ Λ L

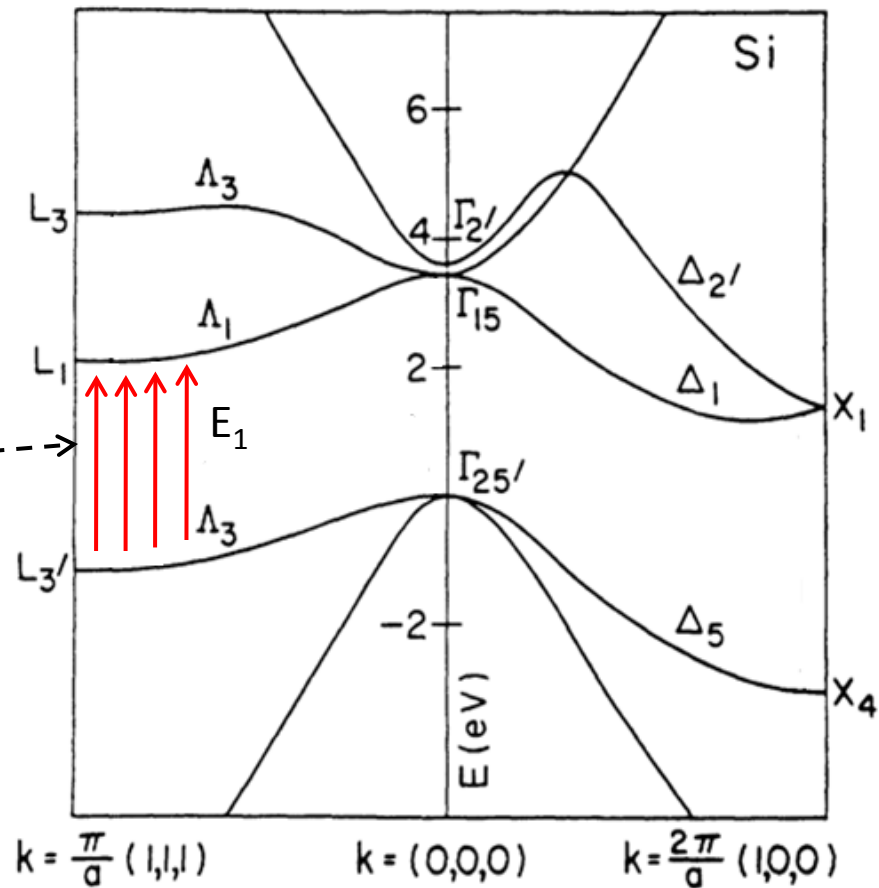
[110] Direction: Γ Σ K



ϵ_2 : Imaginary part of the dielectric function

Critical Point

- Constant energy difference between the valence and conduction band.
- In optical physics terms – a high joint density of states



Band structure of Si calculated from the $\mathbf{k} \cdot \mathbf{p}$ method²

¹C. Kittel, Introduction to Solid State Physics (Wiley, New York, 1996)

²M. Cardona and F. H. Pollak, Phys. Rev. B 142, 530 (1966).



Direct space analysis:

Lorentzian line shape

$$\varepsilon = Ce^{i\beta} (E - E_g + i\Gamma)^{-\mu}$$

Double derivative of the Lorentzian line shape

$$\frac{d^2\varepsilon}{dE^2} = \begin{cases} \mu(\mu+1)Ce^{i\beta} (E - E_g + i\Gamma)^{-\mu-2}, & \mu \neq 0 \\ Ce^{i\beta} (E - E_g + i\Gamma)^{-2}, & \mu = 0 \end{cases}$$

C – amplitude

β – phase factor

E_g – threshold energy (E_{CP})

Γ – lifetime broadening

μ – order of singularity

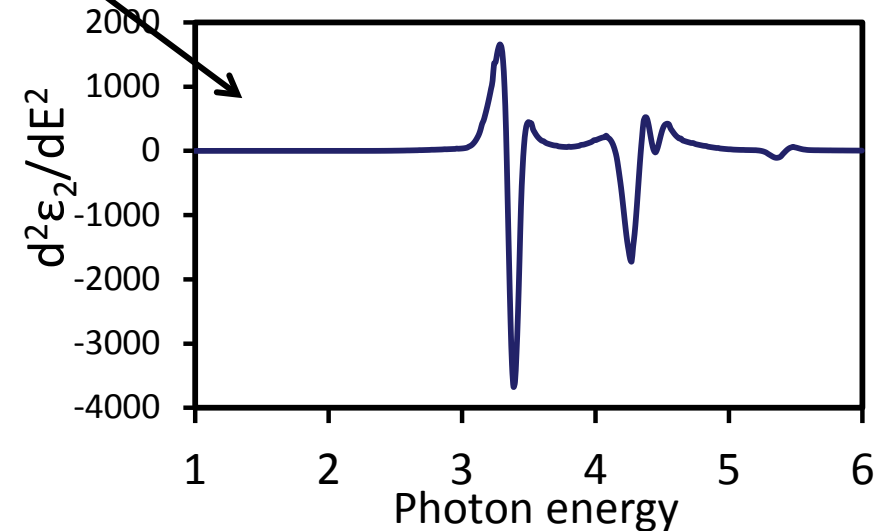
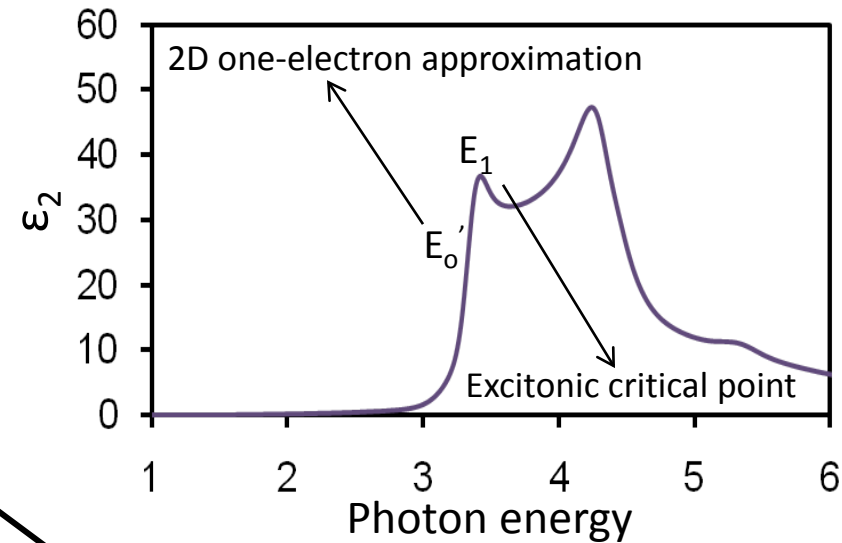
$\mu = \frac{1}{2}$ (3D one-electron approximation)

$\mu = 0$ (2D one-electron approximation)

$\mu = -\frac{1}{2}$ (1D one-electron approximation)

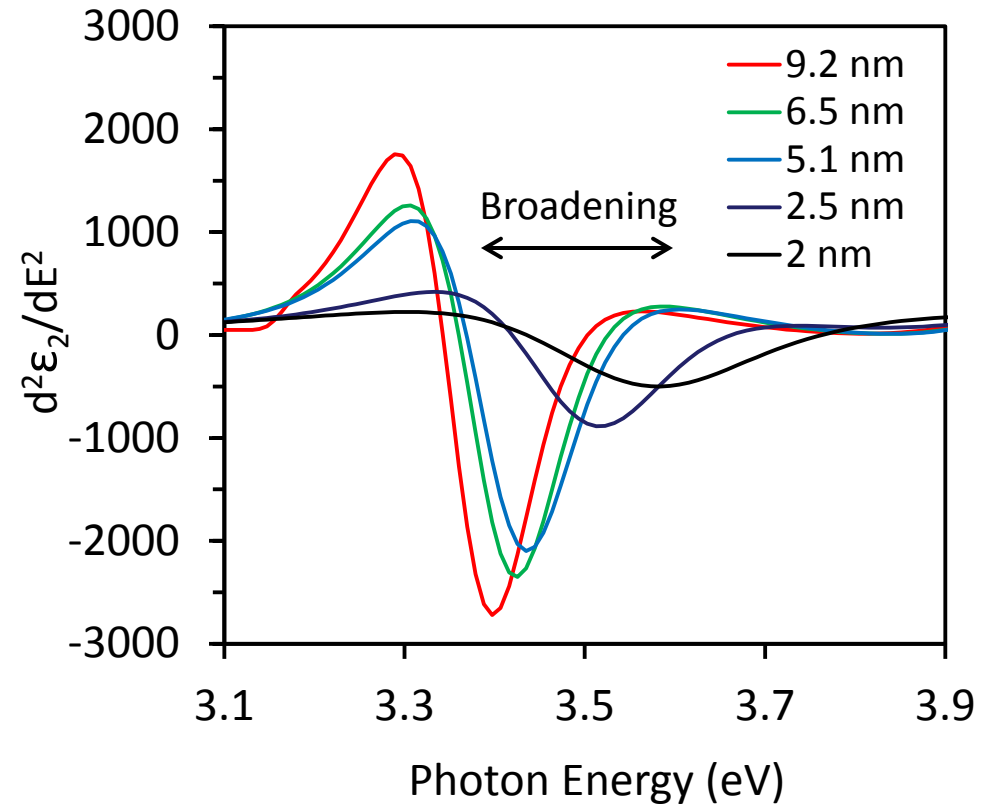
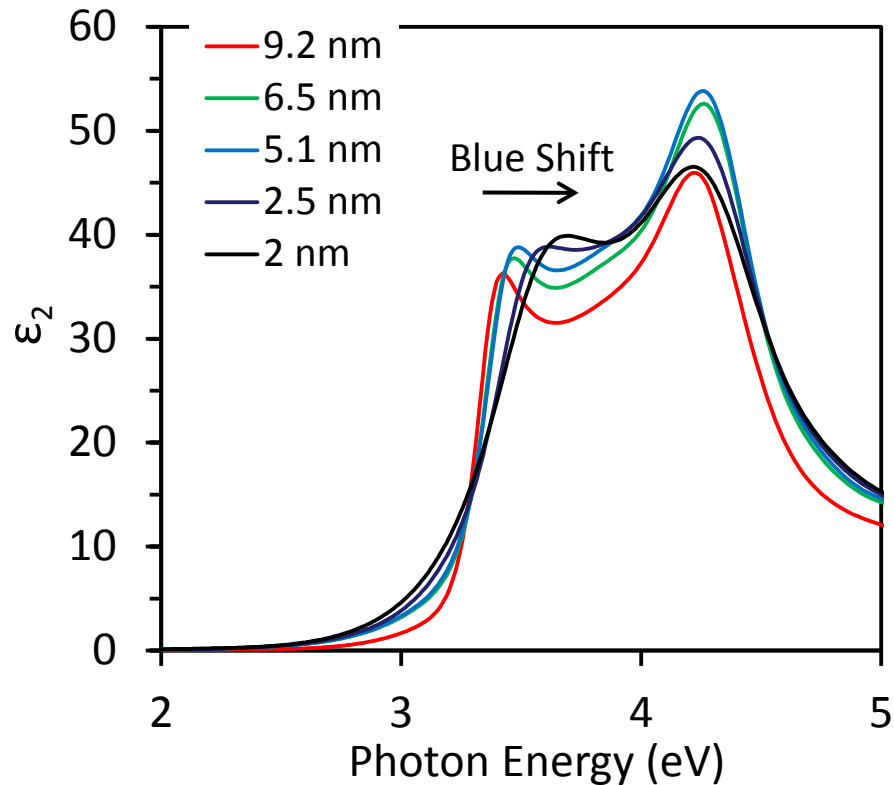
$\mu = 1$ (excitonic critical points)

Dielectric function of Si (experimental):





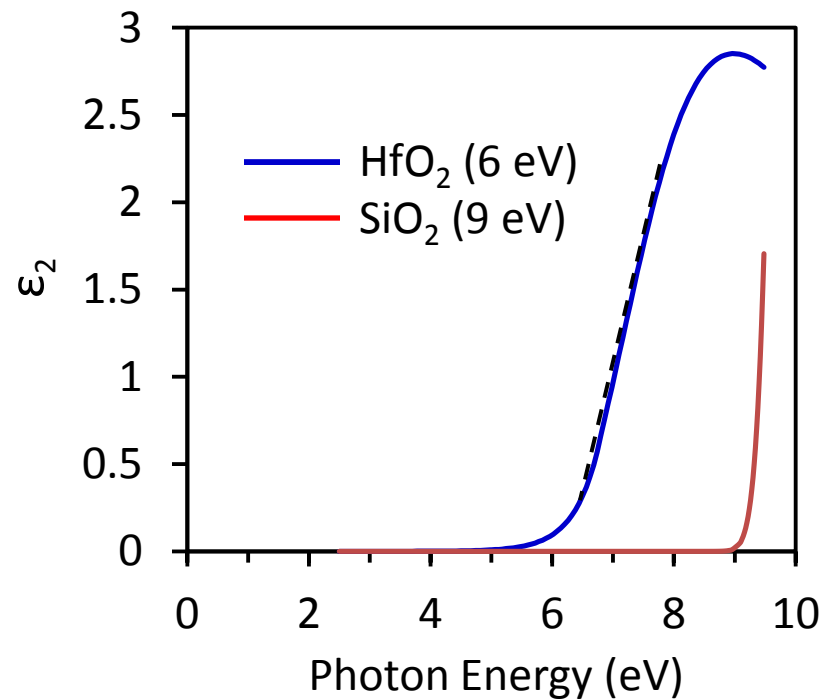
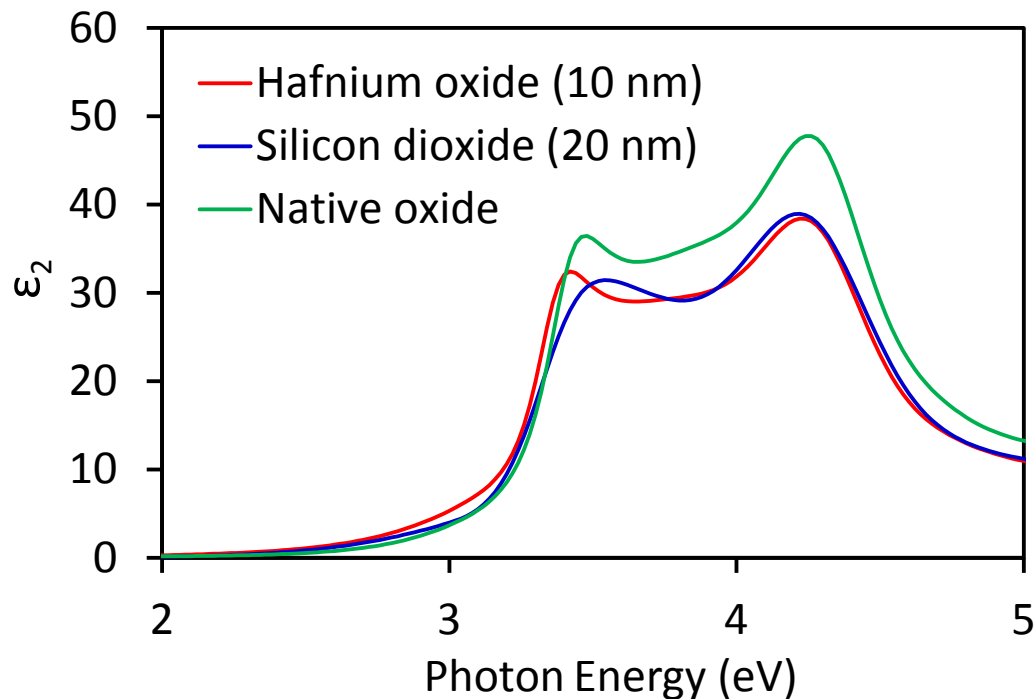
Imaginary part of the dielectric function and its second derivative



- Change in the dielectric function of c-Si nanoscale films at different thickness
- Blue shift in the critical point energy is observed



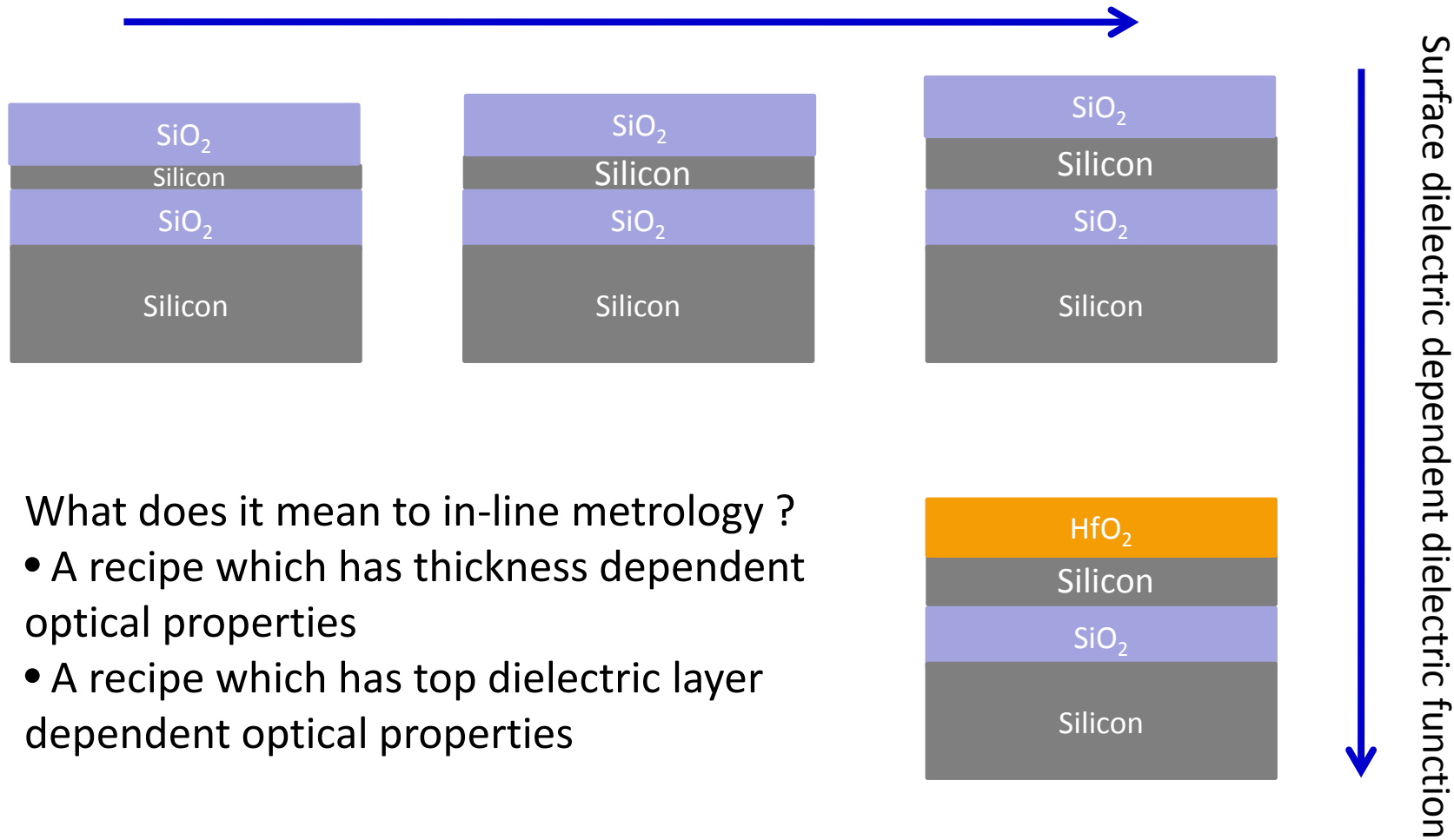
Imaginary part of the dielectric function of *c*-Si QWs (~ 5 nm)



Altering the optical response by changing the top dielectric layer: changes in quantum confinement and electron-phonon interaction



Thickness dependent dielectric function



What does it mean to in-line metrology ?

- A recipe which has thickness dependent optical properties
- A recipe which has top dielectric layer dependent optical properties

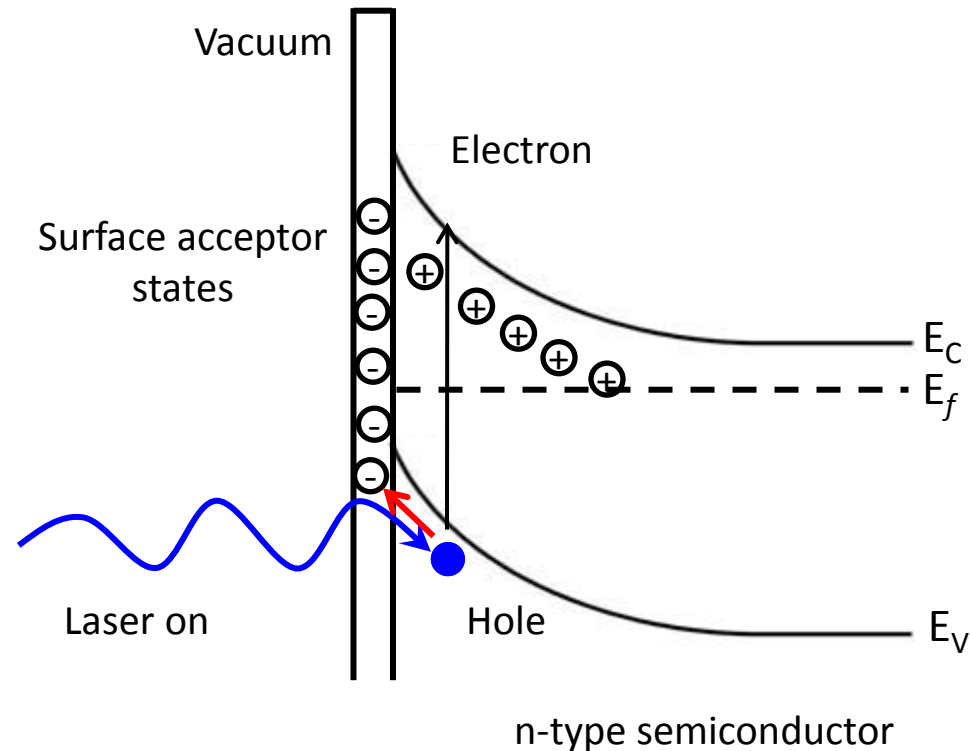


- Linear Optical Response of Materials
- Spectroscopic Ellipsometry
- Advanced Materials in the Semiconductor Industry
- **Photoreflectance**
- Photoluminescence
- Conclusions
- Acknowledgements



Modulation spectroscopy (non-linear optical spectroscopy)

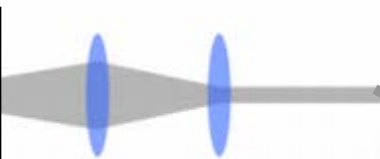
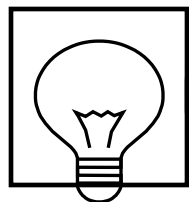
- Space charge layer at the surface due to Fermi level pinning
- Laser light produces carriers
- Carriers neutralize charge at the interface
- Modulation of light alters band bending
- Complex dielectric functions changes with band bending



Complementary technique to measure the shift in the energy and lifetime broadening of the E_1 critical point



Xenon source (probe)



CW Laser

532 nm
(pump)



Chopper

Chopped 1.38 k Hz



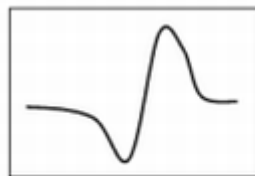
Filter

Monochromator

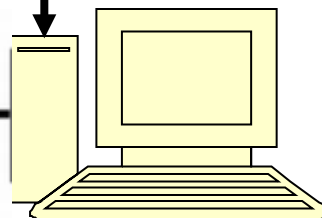
CCD

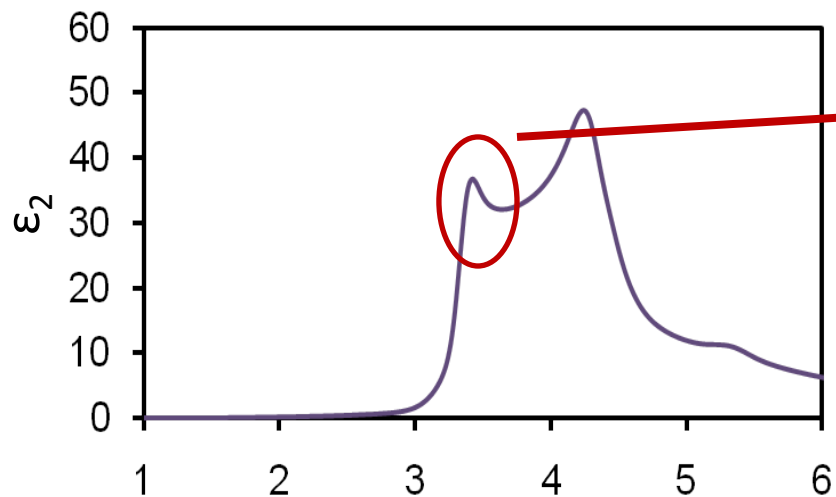
$$\frac{\Delta R}{R}(\hbar\omega) = \frac{R_{off}(\hbar\omega) - R_{on}(\hbar\omega)}{R_{off}(\hbar\omega)}$$

X,Y sample
Stage

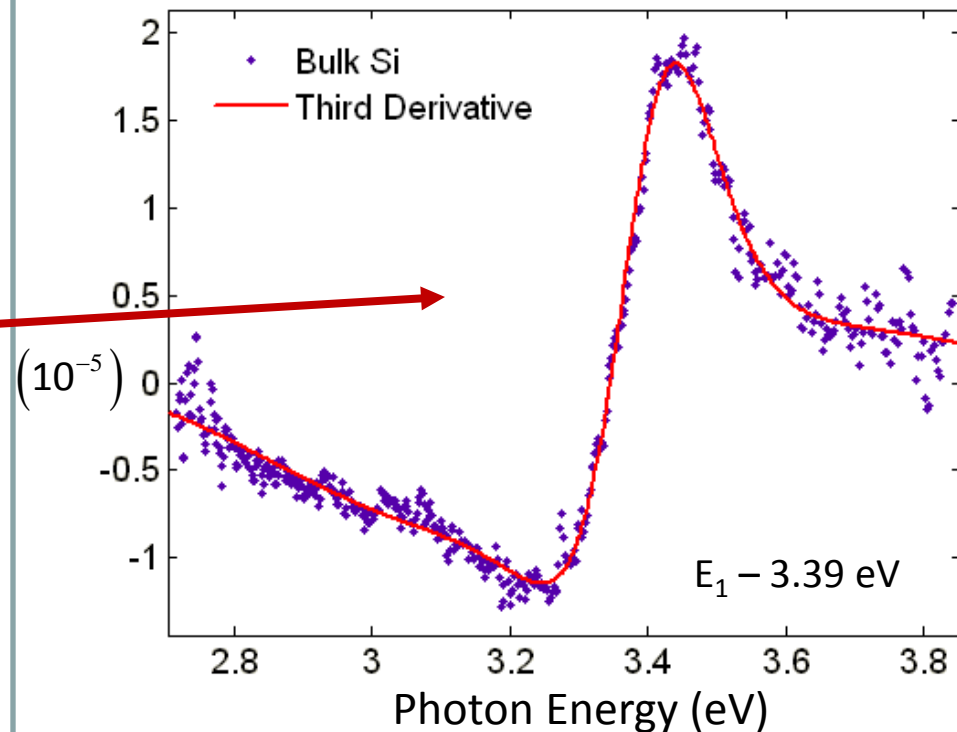


PR Spectrum





Experimental



A: Amplitude

Θ : Phase

E_{CP} : Critical point

Γ : Lineshape Broadening

n: Determined by type of CP

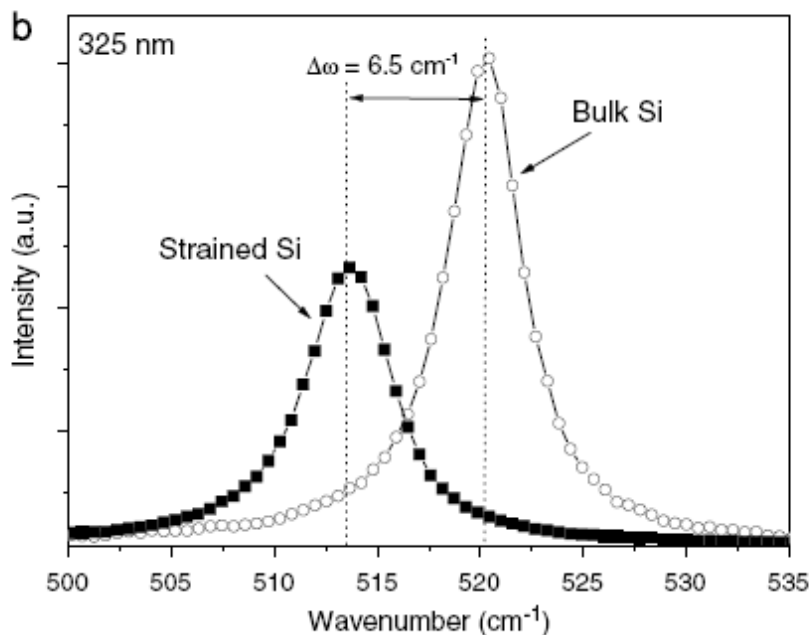


Fig. 1. Raman spectra corresponding to the sSOI sample using visible (514 nm) (a) and UV (325 nm) excitation (b).

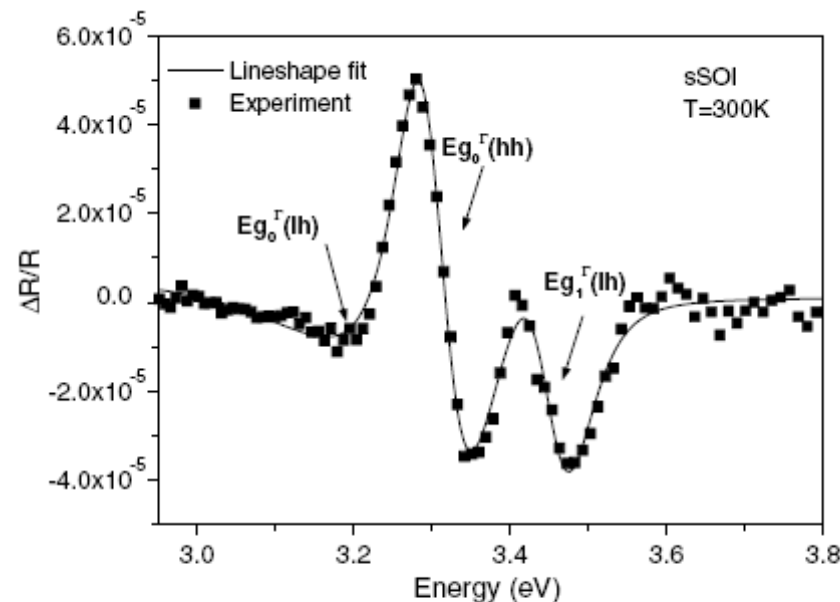
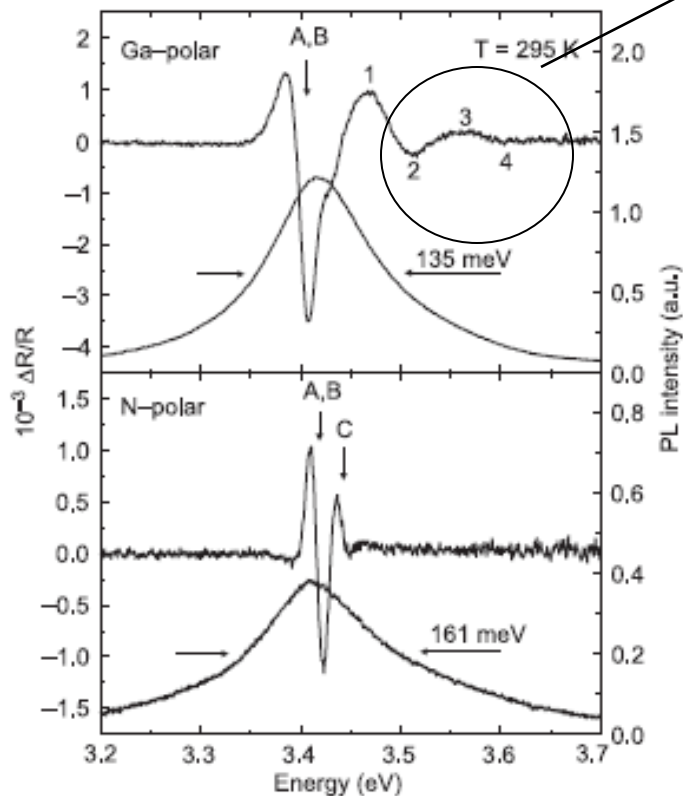


Fig. 4. PR spectrum of strained silicon layer at room temperature (dotted curve). The solid line is corresponds to the theoretical fit.

- Three transitions energies are (i) 3.19 eV, (ii) 3.30 eV and (iii) 3.45 eV.
- Calculations show tensile strain of 1% in the strained Si overlayer
- This value is again in good agreement with the nominal tensile strain and with the values obtained from RS and Low Temp PhotoLuninescence.



Franz Keldysh Oscillations
Due to internal electric field in polar GaN



g. 1. Photoluminescence and photoreflectance spectra of Ga- and N-polar thick GaN layers grown by HVPE.

$$\frac{\Delta R}{R} \propto \exp\left[\frac{-2\Gamma\sqrt{E - E_g}}{(\hbar\theta)^{3/2}}\right] \times \cos\left[\frac{4}{3}\left(\frac{E - E_g}{\hbar\theta}\right)^{3/2} + \phi\right] \frac{1}{E^2(E - E_g)},$$

$$F = \frac{(\hbar\theta)^{3/2} \sqrt{2\mu}}{e\hbar},$$

where $\hbar\theta$ is the electro-optic energy, Γ is the linewidth, ϕ is the phase factor, F is the electric field, and μ is the electron hole reduced mass ($\mu = 0.2 m_0$). The field estimated from the period of FKO is 215 kV/cm (see Fig. 3). Such a huge



Sample	A	B	C	D	E
%Sb	38.3	38	45.7	51	52.5
Thickness d (nm)	41	72	50	72	41
E_{GHH} (eV)	0.730	0.732	0.705	0.694	0.692
E_{GLH} (eV)	0.681	0.681	0.689	0.695	0.696
$\Delta E_{GHH-GLH}$ (meV)	49	51	16	1	4
F (kV/cm)	92	52	80	54	96

Internal
E Field

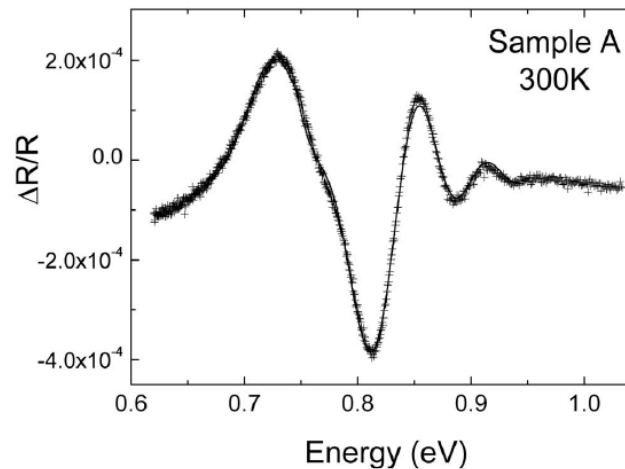
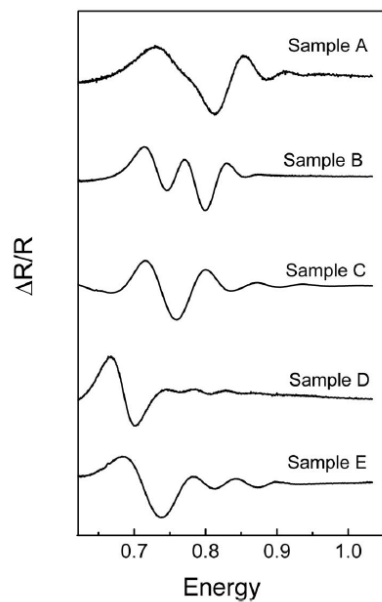


FIG. 1. Room temperature PR spectra for all samples.



- Linear Optical Response of Materials
- Spectroscopic Ellipsometry
- Advanced Materials in the Semiconductor Industry
- Photoreflectance
- **Photoluminescence**
- Conclusions
- Acknowledgements



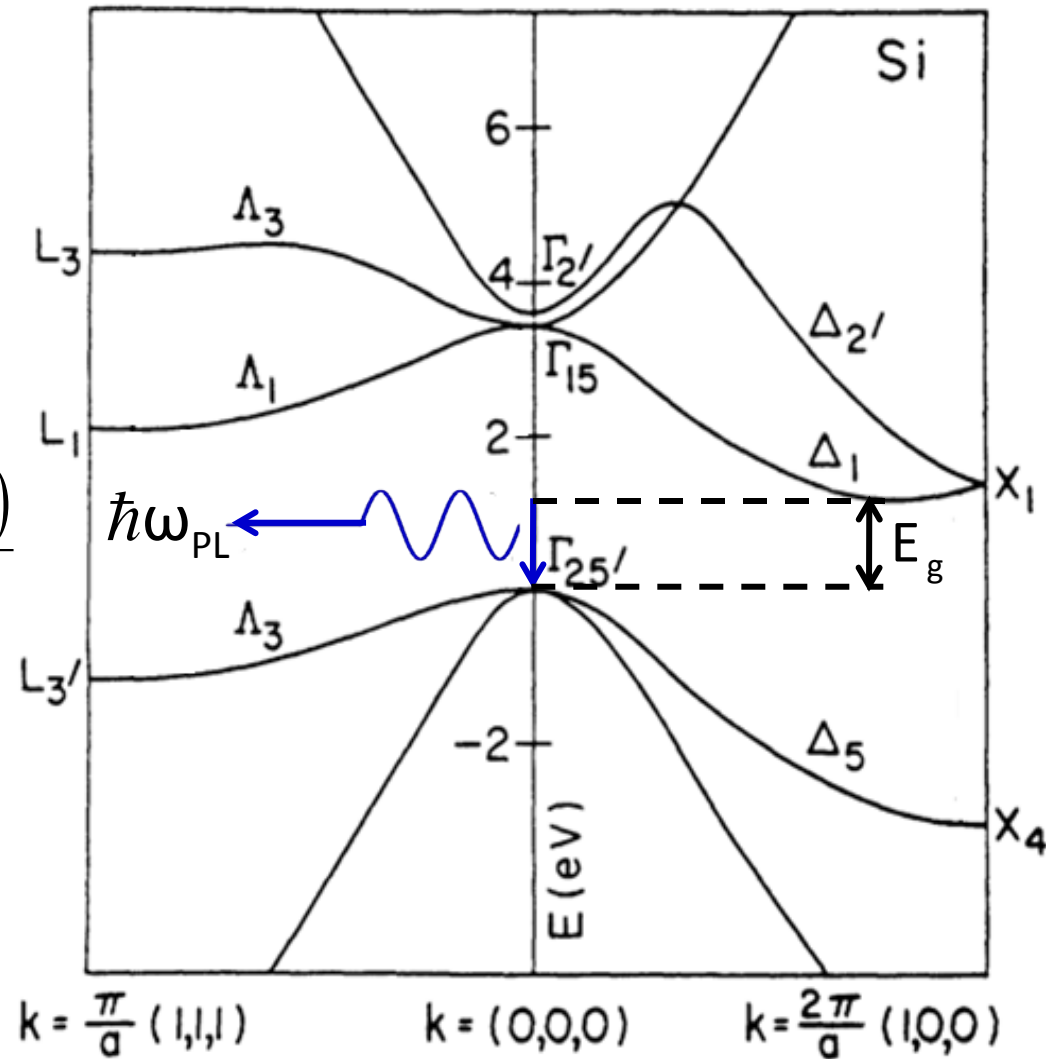
Photoluminescence is used to study the changes in the indirect transitions due to quantum confinement and change in dielectric medium

Photoluminescence peak energy (2D)

$$E = E_{gap} + E_{QC} - \frac{R_y}{\left(n - \frac{1}{2}\right)^2} + \frac{\hbar^2 (k_x^2 + k_y^2)}{2M}$$

$$E_{QC} = \frac{\hbar^2 \pi^2}{2ML^2}$$

$$R_y = \frac{m^*}{2} \left(\frac{e^2}{4\pi\epsilon\hbar} \right)^2 \rightarrow \text{Rydberg}$$

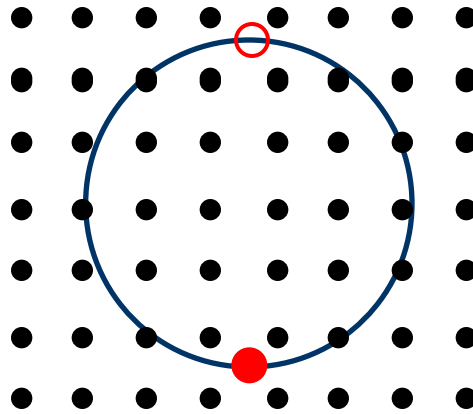


Band structure of Si calculated from the $\mathbf{k}\cdot\mathbf{p}$ method¹

¹M. Cardona and F. H. Pollak, Phys. Rev. B 142, 530 (1966).

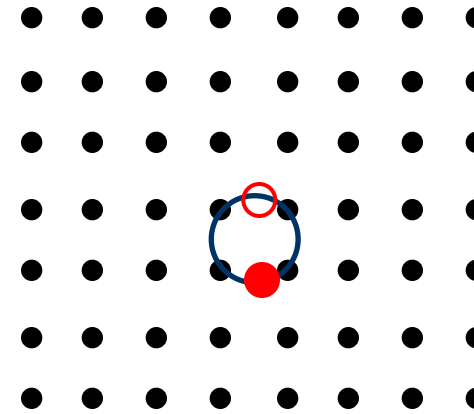


BE ~ 0.01 eV



a) Free Excitons
(Wannier-Mott Excitons)
(Delocalized states)

BE ~ 0.1 to 1 eV



b) Bound Excitons
(Frenkel Excitons)
(Localized states)

$$n \ll \left(\frac{mk_B T}{2\pi\hbar^2} \right)^{\frac{3}{2}} \text{Exp} \left(\frac{-E_g}{2k_B T} \right)$$

As the power is increased, at high densities, and at low temperatures the free excitons condense to form a liquid phase.

This liquid phase manifests itself in the formation of EHD (Electron-hole droplets) – a broad feature in luminescence.

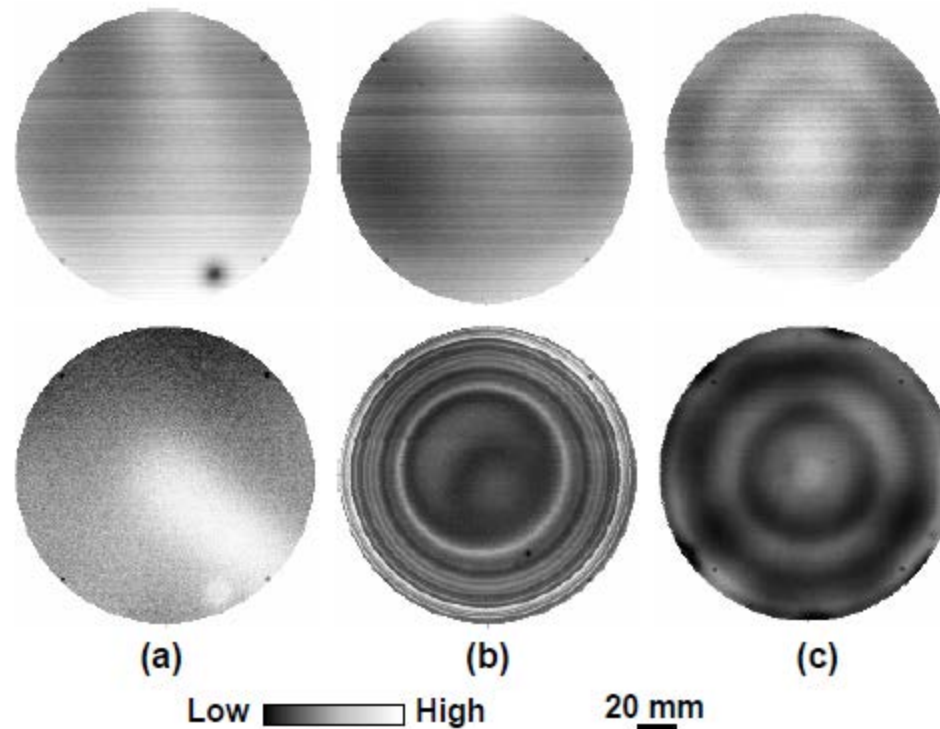


Fig. 2. PL mapping on (a) SIMOX, (b) Unibond[®], and (c) ELTRAN[®] wafers with $t_{\text{SOI}} = 170 - 200$ nm at room temperature: Upper and lower figures are on top Si layers and substrates, respectively.



- Linear Optical Response of Materials
- Spectroscopic Ellipsometry
- Advanced Materials in the Semiconductor Industry
- Photoreflectance
- Photoluminescence
- **Conclusions**
- Acknowledgements



- A wide range of wavelengths makes Spectroscopic Ellipsometry a very powerful method capable of measuring more than just thickness and refractive index
- Non Linear Optical methods such as Photoreflectance and Photoluminescence provide information not available from spectroscopic ellipsometry

